

Colloid Formation Resulting from Alum Coagulation of Organic-Laden Sourcewaters

William Michael Hardin

Thesis submitted to the Faculty of the Virginia
Polytechnic Institute and State University in partial
fulfillment of the requirements for the degree of

MASTER OF SCIENCE

in

Environmental Engineering

William R. Knocke, Co chair

Christopher J. Tadanier, Co chair

Marc A. Edwards

September 10, 2003

Blacksburg, Virginia

Keywords: colloid, natural organic matter, coagulation, alum

Copyright 2003, William M. Hardin

Colloid Formation Resulting from Alum Coagulation of Organic-Laden Sourcewaters

William Michael Hardin

(ABSTRACT)

This research evaluated natural organic matter (NOM) dissolved-solid phase separation resulting from alum coagulation under the following sourcewater conditions: pH, initial NOM concentration, initial turbidity, and temperature. The solid phase was partitioned into two operationally defined size fractions; colloidal matter was defined as organic carbon (OC) retained by a 30 kilodalton ultrafiltration membrane, and particulate matter was defined as OC retained by a 1 μ m glass-fiber filter. Coagulation pH had a considerable impact on residual OC colloid formation, signified by more colloids formed as a function of alum dose at pH 6.8 as compared to pH 5.8. Initial NOM concentration strongly influenced the alum dose range over which OC colloid formation occurred and was found to be a proportional relationship. The presence of bentonite clay (used as the initial turbidity source) somewhat affected OC colloid formation by exerting some amount of coagulant demand, signified by decreasing OC colloid formation with increasing initial turbidity. Coagulation temperature had a considerable impact on particulate matter formation, as there was an increase in the dose at which particle formation first occurred at 4 °C when compared to 25 °C. Phase separation of OC from dissolved to colloidal matter was very similar at both 4 °C and 25 °C. The ability for low doses of polymers to replace a large portion of alum in order to further aggregate colloids during flocculation was unsuccessfully investigated. OC phase separation resulting from alum and iron sulfate coagulation was compared on a molar coagulant metal basis. The amount of residual OC associated with colloidal matter was similar, while the critical coagulant dose at which particulate matter formed was shifted to a much higher dose for iron.

ACKNOWLEDGMENTS

First and foremost, I would like to thank Dr. Knocke for his truly invaluable support and guidance throughout my entire graduate degree program, research and coursework alike. I am convinced that he will prove to be my most important influence in current and future career successes. I would like to thank Dr. Tadanier who provided countless hours of assistance during both the research and writing stages of this work. I would like to thank Dr. Edwards, who rounded out the research committee, for providing crucial expertise in the development of this research.

I would like to thank Erika Masters for her fantastic support as a research partner. I would like to thank Jody Smiley and Julie Petruska for their instrumentation and experimental logistics support. Finally, I would like to thank Betty Wingate and Sherry Burke for their wonderful administrative assistance.

TABLE OF CONTENTS

LIST OF FIGURES	v
LIST OF TABLES	ix
CHAPTER 1: INTRODUCTION	1
CHAPTER 2: METHODS AND MATERIALS	5
2.1 Test Water Make-up	5
2.2 Alum and Polymer Stock Solution Preparation	8
2.3 Jar Testing Procedure.....	8
2.4 Turbidity Measurements	11
2.5 Analysis of Total Organic Carbon	11
2.6 Residual Aluminum Measurements.....	12
2.7 Zeta Potential Measurement	12
2.8 Operationally Defined Size Fractionation.....	12
2.9 Effect of Sulfate Concentration on Coagulation.....	15
CHAPTER 3: RESULTS AND DISCUSSION.....	18
3.1 Phase separation of Organic Carbon and Coagulant Metal	18
3.2 Effect of pH on Colloid Formation.....	20
3.3 Effect of NOM Concentration on Colloid Formation.....	24
3.4 Effect of Initial Turbidity on Colloid Formation	26
3.5 Effect of Coagulation Temperature on Colloid Formation.....	30
3.6 Characterization of Colloid Zeta Potential as a Result of Coagulation	34
3.7 Optimization of NOM Removal Using Polymeric Flocculant Aids.....	36
3.8 Comparison of Colloid Formation Between Alum and Iron Sulfate	37
CHAPTER 4: CONCLUSIONS	47
REFERENCES	49
VITA.....	52

LIST OF FIGURES

- Figure 1. Percent OC recovered for a single NOM stock solution batch during filtration-dialysis using a 30 kDa UF membrane. Each cell pass consecutive to the first involved diluting the retentate of the previous pass as defined elsewhere in the text. 6
- Figure 2. Typical jar test data plotted as residual organic carbon (OC) versus coagulant dose. Solid line indicates OC passing through 1 μ m GF filter; dashed line indicates OC passing through 30 kDa UF membrane. 13
- Figure 3. OC phase separation versus added sulfate. Test water was coagulated with 10 mg/L alum. Nominal test water conditions were pH 5.8, 5 mg/L OC, 0 NTU turbidity (no added bentonite clay), and 25 °C..... 16
- Figure 4. Phase separation of OC (panel A) and residual turbidity (panel B) in relation to coagulant dose. Nominal test water conditions were pH 6.8, 5 mg/L OC, 0 NTU turbidity (no added bentonite clay), and 25 °C. Filled symbols indicate material passing through 1 μ m GF filter, open symbols indicate material passing through 30 kDa UF membrane. 19
- Figure 5. Organic carbon phase separation as a function of alum dose. Nominal test water conditions were pH 5.8, 10 NTU turbidity (bentonite clay), and 25 °C. Test water TOC as indicated in legend. Filled symbols indicate OC passing through 1 μ m GF filter, open symbols indicate OC passing 30 kDa UF membrane. 21
- Figure 6. Organic carbon phase separation as a function of alum dose. Nominal test water conditions were pH 6.8, 10 NTU turbidity (bentonite clay), and 25 °C. Test water TOC as indicated in legend. Filled symbols indicate OC passing through 1 μ m GF filter, open symbols indicate OC passing through 30 kDa UF membrane..... 22
- Figure 7. Residual turbidity as a function of alum dose. Nominal test water conditions were pH 5.8 (panel A), pH 6.8 (panel B), 10 NTU turbidity

	(bentonite clay), and 25 °C. Test water OC ₀ as indicated in legend. envelope shoulders occurred at approximately the same normalized alum dose.	23
Figure 8.	Normalized phase separation of OC as a function of alum dose. Nominal test water conditions were pH 6.8, 10 NTU turbidity (bentonite clay), and 25 °C. Test water OC ₀ as indicated in legend (TOC). Filled symbols indicate OC passing through 1µm GF filter, open symbols indicate OC passing through 30 kDa UF membrane.	25
Figure 9.	Residual turbidity as a function of alum dose. Horizontal axis normalized with respect to initial OC concentration. Nominal test water conditions were pH 6.8, 10 NTU turbidity (bentonite clay), and 25 °C. Test water OC ₀ as indicated in legend (TOC).	27
Figure 10.	Organic carbon phase separation as a function of alum dose. Vertical axis normalized with respect to initial test water OC concentration. Nominal test water conditions were pH 6.8, 5 mg/L OC, and 25 °C. Test water turbidity as indicated in legend. Filled symbols indicate OC passing through 1µm GF filter, open symbols indicate OC passing through 30 kDa UF membrane.	28
Figure 11.	Residual turbidity as a function of coagulant dose. Nominal test water conditions were pH 6.8, 5 mg/L OC, and 25 °C. Test water turbidity as indicated in legend.	29
Figure 12.	Panel A – residual OC as a function of coagulant dose. Vertical axis normalized with respect to OC ₀ . Panel B – residual turbidity as a function of coagulant dose. Nominal test water OC ₀ was 2.5 mg/L. Circles indicate 25 ° C, pH 6.8, test water turbidity was 8.1 NTU. Triangles indicate 4 ° C, pH 7.5, test water turbidity was 10.1 NTU.	31
Figure 13.	Panel A – residual OC as a function of coagulant dose. Vertical axis normalized with respect to OC ₀ . Panel B – residual turbidity as a function of coagulant dose. Nominal test water OC ₀ was 5 mg/L. Circles indicate 25 ° C, pH 6.8, test water turbidity was 9.2 NTU. Triangles indicate 4 ° C, pH 7.5, test water turbidity was 9.9 NTU.	32

Figure 14. Panel A – residual OC as a function of coagulant dose. Vertical axis normalized with respect to OC_0 . Panel B – residual turbidity as a function of coagulant dose. Nominal test water OC_0 was 10 mg/L. Circles indicate 25 ° C, pH 6.8, test water turbidity was 10.1 NTU. Triangles indicate 4 ° C, pH 7.5, test water turbidity was 9.5 NTU.	33
Figure 15. OC phase separation as a function of polymer dose. Panel A – cationic polymers with varying nominal molecular weight (see Table 2). Panel B – nonionic polymers with similar molecular weight (see Table 2). Nominal test water conditions were pH 6.8, 10 mg/L OC_0 , 10 NTU turbidity, and 25 °C.	38
Figure 16. Residual turbidity as a function of polymer dose. Panel A – cationic polymers with varying nominal molecular weight (see Table 2). Panel B – nonionic polymers with similar molecular weight (see Table 2). Nominal test water conditions were pH 6.8, 10 mg/L OC_0 , and 25 °C. Test water turbidity as shown in legend.	39
Figure 17. Comparison of alum and iron sulfate coagulant performance on a molar basis. Panel A - OC phase separation as a function of coagulant metal concentration, panel B - residual turbidity. Nominal test water conditions were 5 mg/L OC_0 , pH 6.8, 10 NTU turbidity, and 25 °C. Circles indicate alum, triangles indicate iron sulfate.	42
Figure 18. Comparison of alum and iron sulfate coagulant performance on a molar basis. Panel A - OC phase separation as a function of coagulant metal concentration, panel B - residual turbidity. Nominal test water conditions were 10 mg/L OC_0 , pH 6.8, 10 NTU turbidity, and 25 °C. Circles indicate alum, triangles indicate iron sulfate.	43
Figure 19. Comparison of alum and iron sulfate coagulant performance on a molar basis. Panel A - OC phase separation as a function of coagulant metal concentration, panel B - residual turbidity. Nominal test water conditions were 5 mg/L OC_0 , pH 5.8, 10 NTU turbidity, and 25 °C. Circles indicate alum, triangles indicate iron sulfate.	44

Figure 20. Comparison of alum and iron sulfate coagulant performance on a molar basis. Panel A - OC phase separation as a function of coagulant metal concentration, panel B - residual turbidity. Nominal test water conditions were 5 mg/L OC_0 , pH 7.5, 10 NTU turbidity, and 4 °C. Circles indicate alum, triangles indicate iron sulfate. 45

LIST OF TABLES

Table 1.	Percent TOC removal requirements as dictated by the U.S.E.P.A. D/DBP Rule (Krasner and Amy, 1995).....	2
Table 2.	Polymers used in this research during applicable experiments.	9
Table 3.	Average zeta potential as a function of jar test stage, alum dose, and test water OC ₀ concentration as noted in table. Nominal test water conditions were pH 6.8, 10 NTU turbidity, and 25 °C. Average was taken from five readings of each sample.	35
Table 4.	Differences in experimental conditions between this research and previous work (Siczka, 1997) in demonstration of polymers to enhance OC phase separation from colloidal to particulate matter. Refer to Table 2 for further details of polymer types.	40

CHAPTER 1: INTRODUCTION

Natural organic matter (NOM) removal from source waters is an important component to consider when implementing drinking water treatment strategies because it is a precursor to the formation of disinfection by-products (DBPs) (Singer, 1994). The Disinfectants/Disinfection By-Products (D/DBP) Rule was implemented in 1998 in an effort to decrease DBP formation within drinking water treatment systems (U.S., 1998). NOM is typically measured as total organic carbon (TOC). Under the D/DBP Rule, the removal of organic carbon (OC) is regulated based on source water characteristics, namely TOC and alkalinity (see Table 1). Coagulation has been a strategy used in drinking water treatment to remove turbidity from source waters, however with the D/DBP Rule in effect, NOM removal is now a key component of coagulation. This shift in treatment strategy, termed enhanced coagulation, involves altering coagulation conditions such as coagulant dose in order to achieve regulated TOC removal, while providing effective turbidity removal (Chaiket *et al.*, 2002; States *et al.*, 2002; Edzwald and Tobiason, 1999; Edwards, 1997; White *et al.*, 1997; Crozes *et al.*, 1995; Krasner and Amy, 1995).

NOM is made up of a heterogeneous mixture of organic constituents, and coagulation is known to preferentially remove certain NOM chemical fractions (Krasner and Amy, 1995). Many mechanisms have been identified as potentially playing a role in the removal of NOM during coagulation including double layer compression, adsorption and charge neutralization, incorporation into a precipitated metal hydroxide phase, and adsorption and interparticle bridging (Tadanier *et al.*, 1997). Aluminum sulfate (alum) is widely used in coagulation for the removal of NOM from source waters (Licsko, 1997; Licsko, 1993). The dominant mechanism responsible for NOM removal using alum is adsorption on amorphous aluminum hydroxide particles (Edzwald, 1993). Interactions between NOM and aluminum exist in the form of complexation, and have been extensively studied (Gregor *et al.*, 1997; Hawke *et al.*, 1996; Powell and Hawke, 1995; Plankey, 1995; Brown and Driscoll, 1993; Plankey and Patterson, 1987).

Table 1. Percent TOC removal requirements as dictated by the U.S.E.P.A. D/DBP Rule (Krasner and Amy, 1995).

Raw Water TOC (mg/L)	Raw Water Alkalinity (mg/L as CaCO ₃)		
	< 60	60 - 120	> 120
< 2	no removal required		
2 - 4	35	25	10
4 - 8	45	25	25
> 8	50	40	30

Many source water characteristics can affect coagulation performance in terms of NOM removal. It is generally observed that the coagulation and resulting removal of NOM using alum is optimized in a pH range of 5.5 – 6.0 (Carlson and Gregory, 2000). The chemical characteristics of the NOM are important as only a certain fraction is readily removed through coagulation (Bose and Reckhow, 1998). Furthermore, NOM and aluminum undergo complexation, which is responsible for a majority of the coagulant demand (Carlson and Gregory, 2000). Coagulation temperature has been shown to affect the flocculation and settling properties of treatment as well (Knocke *et al.*, 1986)

Conventional coagulation is aimed at using a coagulant dose that enables particulate matter formation sufficient in size to settle out of solution or be retained by a filter within the treatment plant. At such a dose, a certain fraction of OC is phase separated from a dissolved state into particulate matter, and subsequently removed from the source water (Siczka, 1997). Under lower coagulant dose conditions an intermediate step exists where dissolved OC is phase separated into aggregates not quite large enough to be removed through settling or filtration. This size fraction is typically defined as colloidal matter. The source water and treatment conditions under which NOM associated colloidal matter is formed are not well defined through previous research. Further investigation of these conditions has been suggested (Knocke *et al.*, 1994; Tadanier *et al.*, 1997).

The notion of OC phase separation into colloidal and particulate size fractions leads to a proposed methodology, whereby polymers are used in an unconventional manner to further aggregate colloidal matter formed at low coagulant doses into particles of sufficient size for removal through settling or filtration. For many water treatment utilities, the annual cost of chemicals far surpasses annual energy and labor costs during drinking water treatment (Harms, 1987). The primary goal of this proposed strategy would be the optimization of NOM removal with respect to primary coagulant dose in a cost effective manner, while meeting TOC reduction dictated by the D/DBP Rule. Polymers currently have a role in water treatment, either as primary coagulants or as coagulant and flocculant aids (Lee *et al.*, 1998). Coagulant aids promote increased strength and density of floc, while flocculant aids promote floc growth through

interpartical bridging. The primary difference between the latter and the proposed strategy is the size of solid phase NOM aggregates undergoing further aggregation.

The specific research objectives of this study were: 1) document OC phase separation from dissolved to colloidal and particulate matter resulting from alum coagulation under the following varied test water conditions: pH, NOM concentration, turbidity, and temperature, 2) investigate the use of varied molecular weight cationic and anionic polymers as flocculant aids in order to demonstrate optimization of OC removal with respect to coagulant dose, 3) evaluate relative performance of alum and iron sulfate for OC phase separation on a comparative molar metal basis.

CHAPTER 2: METHODS AND MATERIALS

2.1 Test Water Make-up

All water samples used in jar tests (henceforth termed *test water*) were prepared in the laboratory in order to ensure control over variable and constant conditions. Test samples were prepared approximately twelve hours prior to conducting each jar test in batch form within a 10L Nalgene® carboy. The ingredients for the test water were: reagent water, sodium bicarbonate (NaHCO_3), calcium chloride (CaCl_2), sodium chloride (NaCl), natural organic matter (NOM), and bentonite clay (in those experiments involving turbidity effects). All chemicals used were certified A.C.S chemical grade.

Ultra-pure reagent water was used to ensure minimum contamination of NOM from an outside source (nominal TOC of $50\mu\text{g/L}$). Reagent water was Type I classification obtained from a NANOPure¹ system. The source water to the NANOPure system was distilled and deionized.

Background ions were added in order to simulate representative natural source water conditions. These target conditions were 2.0 meq/L of alkalinity, 0.5 meq/L of hardness, and 0.01 mol/L ionic strength, and were achieved by adding NaHCO_3 , CaCl_2 , and NaCl , respectively.

An NOM stock solution was prepared for the addition of NOM to the test water. NOM was obtained from the International Humic Substances Society (IHSS)² in a freeze-dried form. The dried NOM (2 g) was dissolved in 1 L of reagent water containing the background ions (dilution water). Filtration-dialysis was performed using a 30 kilodalton (30 kDa) ultrafiltration membrane³ in order to remove NOM initially associated with colloidal matter in the IHSS material. Initial analysis of the filtration-dialysis process indicated that approximately seventy percent of the initial TOC was recovered after three passes for a single batch of NOM stock solution, as shown in Figure 1. Nearly eighty-

¹ Model No. D4744, Barnstead, Dubuque, Iowa

² Suwannee River NOM reverse osmosis isolation, catalogue no. 1R101N, IHSS, St. Paul, Minn.

³ YM-30 63.5 mm diameter, Amicon, Beverly, Mass.

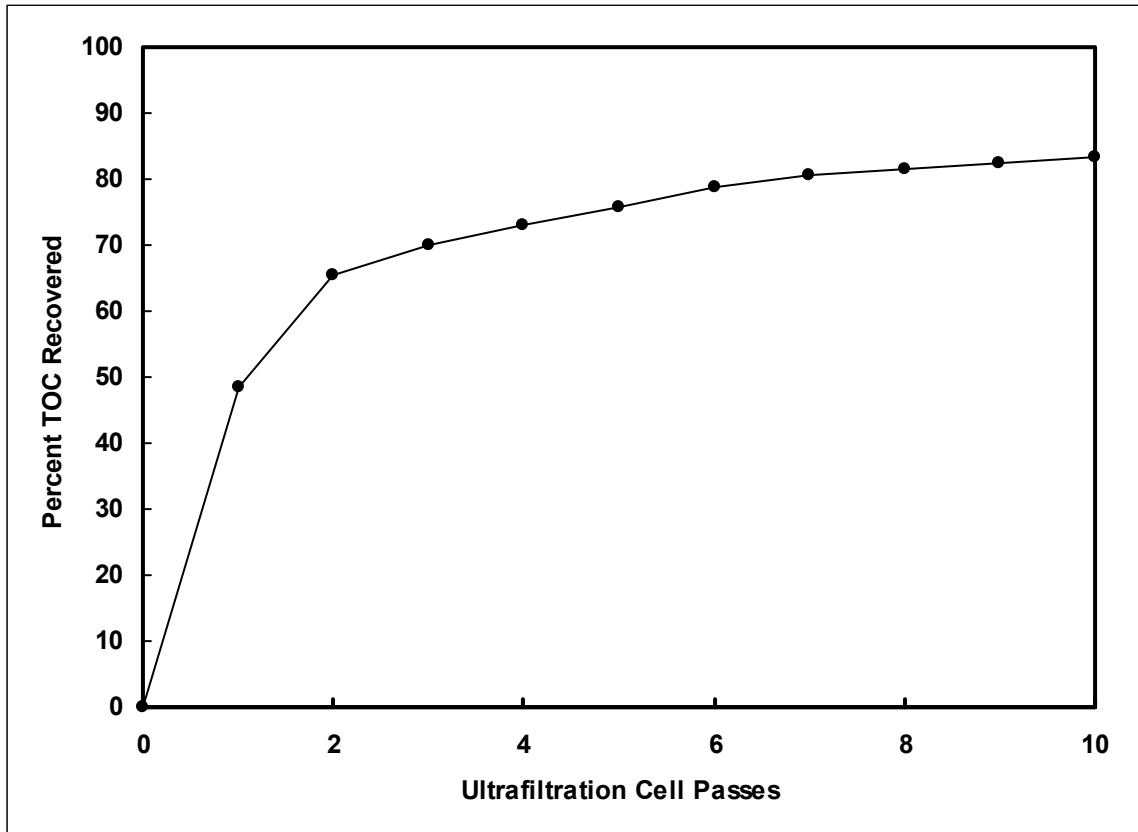


Figure 1. Percent OC recovered for a single NOM stock solution batch during filtration-dialysis using a 30 kDa UF membrane. Each cell pass consecutive to the first involved diluting the retentate of the previous pass as defined elsewhere in the text.

five percent recovery was possible after ten passes and was defined as the total recoverable NOM following ultrafiltration. A single batch of NOM stock solution was defined as the volume of stock solution filling an ultrafiltration cell (volume approximately 200 mL). A pass was defined as pressurizing the ultrafiltration cell and allowing approximately 150 mL to pass through the membrane. Consecutive passes were performed on a single batch by diluting the retentate with dilution water to the full-cell volume, pressurizing the cell, and allowing 150 mL to pass through the membrane. The total collective permeate of three membrane passes, that for all batches of the initial NOM stock solution, was combined into one aliquot, and then a rotovap was used to evaporate enough water to bring the working NOM stock solution down to approximately 1 liter. The nominal TOC of the working NOM stock solution was 850 mg/L and represented approximately eighty-five percent of the 30 kDa recoverable NOM. Three nominal test water initial TOC concentrations were examined in this research: 2.5, 5, and 10 mg/L, which fall within the three TOC ranges set forth by the D/DBP Rule (see Introduction).

Bentonite clay was used to add turbidity to test waters that were expected to contain a targeted initial turbidity. A Bentonite stock solution was made by suspending 10 grams of dry bentonite into 1 liter of dilution water. Intense mixing was imparted using a sonifier⁴ to ensure the bentonite was completely suspended and to break up any aggregation that may have occurred in the stock solution. The bentonite stock was sonified for five minutes immediately before adding bentonite stock each time test waters were prepared.

The pH of test water samples was adjusted with 1 N NaOH and 1 N HCl in batch form within 1 hour prior to conducting each jar test. Two coagulation pH values (5.8 and 6.8) were chosen for comparison in this research. The optimum pH range for NOM removal using alum that is generally observed is 5.5-6.0 (Carlson and Gregory, 2000), giving rise to the first pH value chosen. However, many surface waters that provide a source to municipalities have a pH range much closer to 7.0. Thus, the second pH value was chosen to reflect treatment performance that might occur when coagulating under near-neutral pH conditions.

⁴ Model No. 250, Branson, Danbury, Conn.

2.2 Alum and Polymer Stock Solution Preparation

Alum stock solutions were prepared by adding reagent grade alum⁵ ($\text{Al}_2(\text{SO}_4)_3 \cdot 18 \text{H}_2\text{O}$) to reagent water and stored in high-density polyethylene bottles at ambient laboratory temperature. The concentration of aluminum was sufficiently high that the pH values were less than 2. All alum stock solutions were used for approximately one month each and no visible precipitates were formed in this suspension during that period.

Five polymers were used in selected jar tests, chosen for their varying charge and nominal molecular weights, as shown in Table 2. The neat polymer solution provided by each manufacturer was diluted to a working stock solution so that volumes added during jar tests ranged from approximately 1 – 5 mL. The following procedure was per the manufacturer's recommendations. Based on the specific gravity, the amount of neat polymer solution required to bring 297 mL of reagent water to a 1% (weight/weight) stock solution was weighed into a plastic syringe. Using a hand blender⁶, the neat polymer solution was injected into the vortex shoulder of the reagent water and mixed on high speed for approximately 12 seconds. This mixing intensity provided enough energy to break up the emulsion of the neat polymer solution, while not shearing the polymer molecules themselves. The solution was aged for 30 minutes and then diluted with reagent water to the final working stock solution. TOC of the working stock solution was analyzed to ensure that the polymer concentration was appropriate for use in experimental tests (carbon in the polymer molecules was assumed to be 50% weight/weight).

2.3 Jar Testing Procedure

Jar tests consisted of five stages. The first stage was 2 minutes of rapid mix at 100 rotations per minute (RPM). This was followed by 30 minutes of tapered flocculation, which consisted of three stages at 10 minutes each with paddle speeds of 40,

⁵ Catalogue # 22761-7, Sigma-Aldrich, Inc., St. Louis, Missouri

⁶ Model 1106757, GE, Bentonville, Arka.

Table 2. Polymers used in this research during applicable experiments.

Manufacturer*	Polymer	Classification	Charge	Nominal size (amu)
Cytec	Superfloc® C-572	Coagulant Aid	Cationic	30,000
Cytec	Superfloc® C-581	Coagulant Aid	Cationic	250,000
Cytec	Superfloc® C-4514	Flocculent Aid	Cationic	16,000,000
Cytec	Superfloc® N-1986	Flocculent Aid	Nonionic	16,000,000
Ondeo Nalco	Pol-E-Z 652®	Flocculent Aid	Nonionic	> 10,000,000

* Cytec Industries, Inc., West Paterson, New Jersey

* Ondeo Nalco Company, Naperville, Illinois

30, and 20 RPM. The final stage was 1 hour of settling. Tests were performed using either a PB-700 Jartester⁴ or a Model 300 six paddle stirrer⁷. Plastic jar testing jars with a square cross-section (1 L) were filled with 0.6 L of test water. The water depth within each jar was approximately 12 cm, and the bottom edge of the paddle (width approximately 3 cm) was placed at 25% of the water depth from the bottom of the jar for all experiments. Plastic weigh boats attached to a rod supported above the jars were filled separately with the proper alum dose and a stoichiometric amount of 1 N NaOH required to neutralize the acidic effect of the alum. At the beginning of rapid mix, the rod was rotated so that the alum and NaOH were simultaneously delivered into the vortex of each jar. Immediately following, a small jet of reagent water was used to force any remaining alum or NaOH into the vortex. The pH was monitored for the targeted test water value and necessary adjustments were made using 0.1 N NaOH or 0.1 N HCl within the first 10 minutes of flocculation. The paddles were removed at the beginning of the settling period. After settling, turbidity samples were collected by slowly drawing approximately 20 mL of the supernatant into a wide-mouth pipette at a depth of approximately 1 cm from the free surface. The supernatant was then carefully poured, so as to minimize agitation, into 500 mL amber glass jars for pH measurement and further sample processing.

Jar tests were conducted at two temperature values, 25 °C, and 4 °C, chosen to reflect the typical range of temperature conditions encountered by many municipalities. Jar tests at the higher temperature range were conducted at ambient laboratory temperature, which varied from 22 – 25 °C with an average temperature of 24 °C. Cold water jar tests were conducted by placing two six-paddle stirrers in a tub filled with tap water, 8 lbs. of ice, and copper tubing through which flowed antifreeze chilled at –8 °C. The testing jars were supported so that they were partially submerged in the surrounding chilled tap water sufficient for the test water to maintain ≤ 4 °C, where they remained through settling. The 500 mL amber glass jars containing the supernatant were kept in a 4 °C and were retrieved for individual processing. Previous work has shown that aluminum solubility changed with temperature at constant pH but did not change at constant pOH (Van Benschoten et al., 1992). In this study, test water pOH was the same

⁷ Phipps and Bird, Richmond, Virg.

for experiments at both temperatures, which changed the pH values as determined by the Van't Hoff relationship. The pH values were 6.5 and 7.5 for experiments performed at 4 °C, as compared to pH 5.8 and 6.8 at 25 °C.

An additional step was added to those experiments that examined the use of polymers. Polymer stock was slowly added to the supernatant during flocculation using a 25 mL wide-mouth pipette to ensure even distribution. C-4514 and N-1986 (see Table 2) were added at the beginning of third-stage flocculation, while all others were added at the beginning of first-stage flocculation. The polymer stock solution was mixed at slow speed using a magnetic stir bar prior to each jar test.

2.4 Turbidity Measurements

Turbidity samples were obtained from the supernatant immediately following the settling stage. Approximately 20 mL were slowly drawn into a wide-mouth pipette in order to minimize floc disturbance. The sample was then transferred to a glass cuvette, which was wiped clean with a disposable lens cloth for analysis. Each sample was gently inverted three times just before analysis in order to resuspend any particles that may have settled in the cuvette. Residual turbidity was analyzed using a Turbidimeter Model No. 65⁸. Test water turbidity samples were collected from the carboy in the same manner prior to performing each jar test, and were analyzed along with the residual turbidity samples.

2.5 Analysis of Total Organic Carbon

The test water, residual 1 µm GF filtrate and residual 30 kDa UF permeate samples were collected in 40 mL glass vials and sealed with Teflon lined septa. Total organic carbon (TOC) was measured using an ultra-violet promoted persulfate oxidation method with either a Sievers TOC analyzer⁹ or a Dohrman automated laboratory TOC analyzer¹⁰. The Sievers analyzer measured inorganic carbon and total carbon, and the

⁸ Orbeco-Hellige, Farmingdale, New York

⁹ Model 800 with auto sampler, Boulder, Colo.

¹⁰ Model DC-80, Dohrman/Xertex Corp., Santa Clara, Cal.

difference was recorded as TOC. When using the Dohrman analyzer, samples were first acidified with one drop of 85% phosphoric and sparged with oxygen in order to remove inorganic carbon. The samples were then analyzed for TOC. Each sample was analyzed in triplicate and the average TOC was recorded.

2.6 Residual Aluminum Measurements

Jar tests that did not contain added bentonite clay were analyzed for residual aluminum, as bentonite addition was determined to cause aluminum contamination. Residual 1 μm GF filtrate and residual 30 kDa UF permeate samples were collected in 25 mL HDPE bottles, then acidified with 2 drops of concentrated nitric acid. Residual aluminum was analyzed using a graphite furnace atomic absorption spectrophotometer¹¹. The linear detection range was approximately 1 – 50 $\mu\text{g/L}$, and samples were diluted with reagent water until they were measured within that range.

2.7 Zeta Potential Measurement

Zeta potential of selected jar tests was measured using laser Doppler velocimetry with a Malvern Instruments Zetasizer¹². Samples were carefully drawn into a 20 mL plastic syringe directly from the jar test supernatant, and injected into the zetasizer within two minutes. Zeta potential values were recorded as the average of five measurements.

2.8 Operationally Defined Size Fractionation by Filtration

In this research, operationally defined phase separation of material was based on membrane filtration. Three definitions were formulated for material transitioning from aqueous to solid phases, namely, dissolved, colloidal, and particulate. Figure 2 shows in schematic form a typical data presentation that would be generated by jar testing. These data were based on OC separation, but could be based on other water quality parameters

¹¹ Zeeman 5100 PC, Perkin-Elmer, Norwalk, Conn.

¹² Model 3000 HS, Malvern, Worcestershire, UK

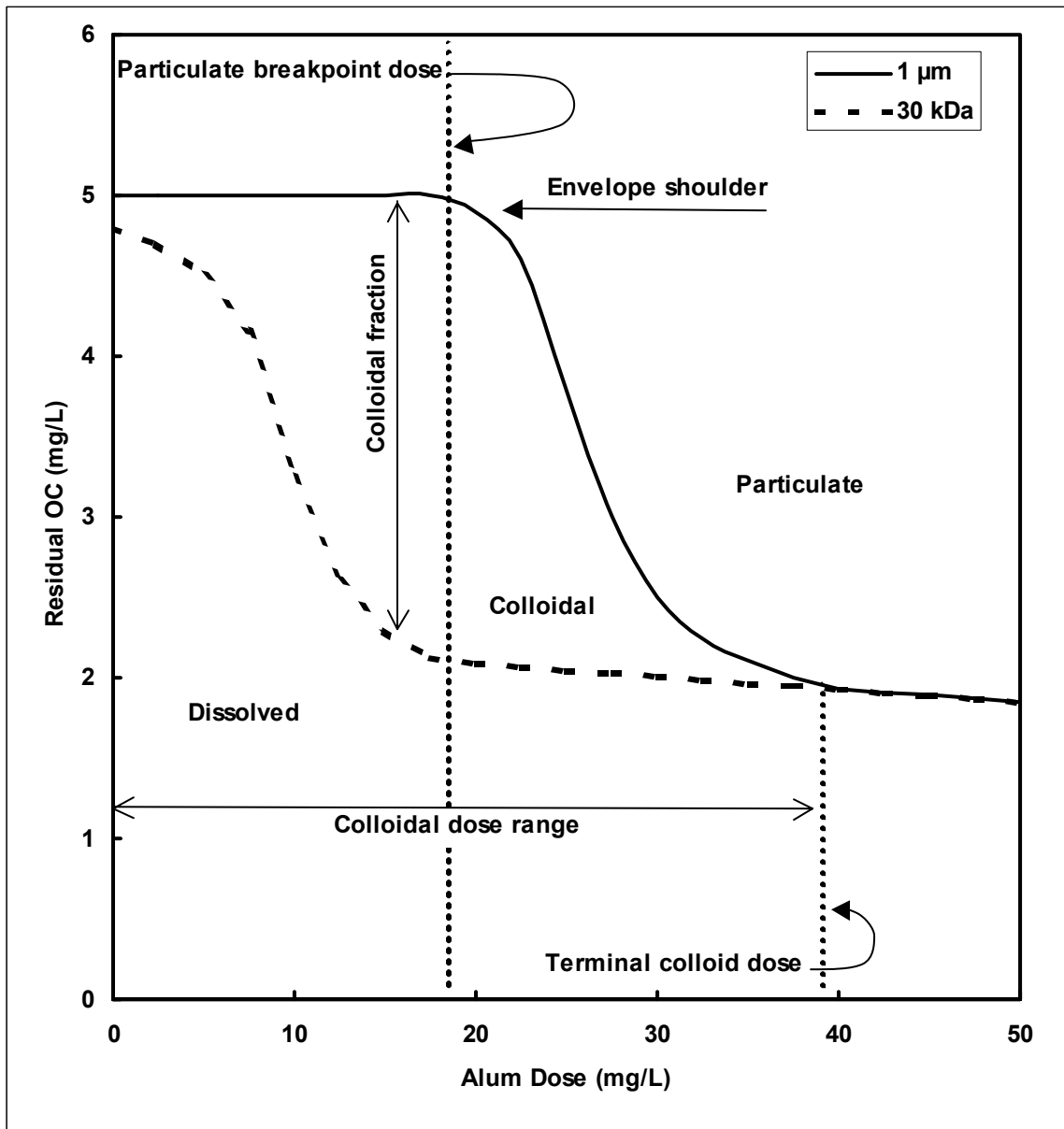


Figure 2. Typical jar test data plotted as residual organic carbon (OC) versus coagulant dose. Solid line indicates OC passing through 1 µm GF filter; dashed line indicates OC passing through 30 kDa UF membrane.

as well. The hypothetical data shown represent residual jar test results, meaning that they are processed from the settled water supernatant after coagulation and flocculation.

The solid line indicates the portion of organic matter (OM) retained by a 1 μm glass-fiber (GF) filter¹³, defined as *particulate OM*. Each filter was cleaned prior to sample processing in order to prevent OC contamination. One liter of distilled/deionized water was passed through each filter followed by 250 mL of reagent water, which was sufficient for OC removal (determined by experimentation). Each sample was passed through a filter by pulling it into a 500 mL vacuum flask, and then a 40 mL sample was obtained for TOC analysis.

The dashed line indicates the portion of the OM that passed through a 30 kilodalton (kDa) ultrafiltration (UF) membrane, defined as *dissolved OM*. Sample filtration was done in series by passing the 1 μm filtrate of each sample through a 30 kDa UF. In order to prevent OC contamination, new membranes were cleansed before use by soaking them in 200 mL of reagent water at twenty-minute intervals for at least one hour. The membranes were then stored in reagent water overnight. The membranes were flushed prior to sample processing to ensure proper working order, which was based on the flux of solution passing through the UF cell. This was accomplished by passing three aliquots (approximately 180 mL each) of reagent water through the cell; the first contained 5 mL 1 N sodium hydroxide, and the second contained 5 mL pH 7.00 phosphate buffer. The flux was measured after flushing and if it was within the manufacturer's range then the membrane was used; if not the membrane was discarded. Membranes were stored in reagent water at 4 °C when not in use.

Organic matter that passes through a 1 μm GF filter but is retained by a 30 kDa UF membrane is defined as *colloidal OM*, and the area enclosed by these lines is termed the *colloidal envelope region*. The *colloidal dose range* occurs over the entire dose range at which the colloidal envelope region is observed. At any given coagulant dose, the amount of colloids formed is termed the *colloidal fraction* and is signified by the separation of the particulate and dissolved organic matter (1 μm and 30 kDa lines, respectively). As coagulant dose increases the colloidal fraction initially increases, then decreases rapidly at doses above the colloidal envelope *shoulder*. At this dose, termed

¹³ A/E 47 mm diameter, Pall Gelman, Ann Arbor, Mich.

the *particulate breakpoint dose*, there is a shift in phase separation where colloidal material is further aggregated into particulate matter. The colloidal fraction ultimately approaches 0 (i.e. the 1 μm and 30 kDa lines come together) at high coagulant doses. However, in some instances a jar test does not capture the entire colloidal envelope, signified by the colloidal fraction not reaching zero. Therefore, the coagulant dose at which the colloidal fraction becomes less than or equal to 2 % of the TOC content is termed the *terminal colloid dose*.

2.9 Effect of Sulfate Concentration on Coagulation

Previous work in water without NOM has shown that at pH range 5.6 – 6.2, 30 mg/L sulfate was sufficient to shift aluminum from soluble to an insoluble form (Kvech and Edwards, 2002). OC phase separation into particulate matter during alum coagulation relies on the formation of aluminum hydroxide aggregates resulting from aluminum insolubility. With varying alum doses, and conjunctively with varying sulfate doses, it was important to ensure there was no effect of sulfate on the results presented in this study. The ratio of aluminum and sulfate has also been shown to affect the rate of coagulation, although theoretically the ratio does not change with varying alum dose (Wang et al., 2002).

During the method development stages of this research, an experiment was performed in order to determine the effect of varying sulfate concentration on OC phase separation. This experiment was performed by adding sulfate during rapid mix at the same time and in the same manner as alum (see section 2.3). The sulfate stock solution was prepared using Na_2SO_4 diluted with reagent water. Test water was coagulated with 10 mg/L alum, which contributed approximately 8.5 mg/L sulfate. One jar contained no additional sulfate, while an increasing additional sulfate dose was added to subsequent jars.

Sulfate concentration did not affect phase separation of dissolved NOM into colloidal aggregates if the soluble NOM in solution was at or above 5 mg/L OC. The amount of residual OC partitioned into the colloidal size range was similar over the entire sulfate dose range, as shown in Figure 3. Because no effect of sulfate concentration on

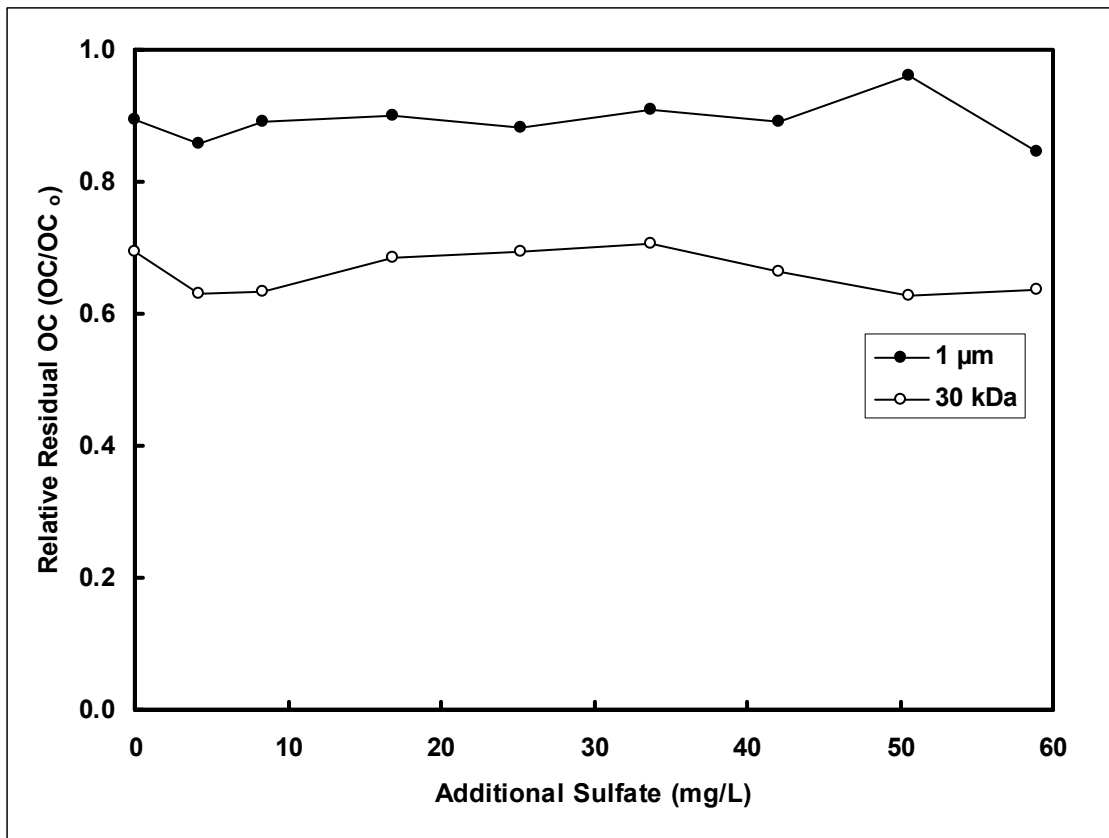


Figure 3. OC phase separation versus added sulfate. Test water was coagulated with 10 mg/L alum. Nominal test water conditions were pH 5.8, 5 mg/L OC, 0 NTU turbidity (no added bentonite clay), and 25 °C.

OC phase separation was observed, it was determined unnecessary to supplement the experiments presented in this research with additional sulfate to some constant level.

CHAPTER 3: RESULTS AND DISCUSSION

The focus of this research was the investigation of colloidal sized particle formation during coagulation as a function of coagulant dose under varying experimental conditions. The terminology introduced in section 2.8 will be used to describe jar test results. First, the notion of colloid formation will be presented. These results demonstrate that coagulant metal was incorporated into colloidal sized aggregates associated with a certain fraction of NOM. The bulk of the results from this research will then be presented and discussed, focusing on varied test water conditions, such as solution pH, NOM concentration, turbidity, and temperature. Zeta potential of the colloids formed during coagulation was measured in order to characterize the negative charge associated with the colloids. Subsequently, polymeric flocculant aids were added in an attempt to enhance removal of the colloidal NOM that was formed at low coagulant doses. Finally, the relative coagulation performance of alum and iron sulfate in terms of dissolved NOM phase separation was examined.

3.1 Phase separation of Organic Carbon and Coagulant Metal

Phase separation of OC is intimately related to that of coagulant metal. This relationship can be seen by examining the residual OC, residual coagulant metal, and the residual turbidity as a function of coagulant dose. For nominal test water conditions of 5 mg/L initial organic carbon (OC_0), pH 6.8, and < 1 NTU turbidity, the maximum colloidal fraction occurred at the same coagulant dose as the peak in residual colloidal aluminum, indicating incorporation of OM and coagulant metal in colloidal aggregates, as illustrated in Figure 4A. Furthermore, at this coagulant dose and lower doses virtually all added coagulant metal was incorporated in colloidal matter.

Residual turbidity was also strongly correlated with residual aluminum, as shown in Figure 4, panel B. The colloidal aluminum and residual turbidity peaks occurred at the same alum dose, which corresponded to the dose of maximum incorporation of OC in colloidal matter. Similarly, at higher coagulant doses residual aluminum and turbidity levels decreased proportionally, again indicating the apparent link between formation of colloidal matter and residual particulate aluminum. Little aluminum was associated with

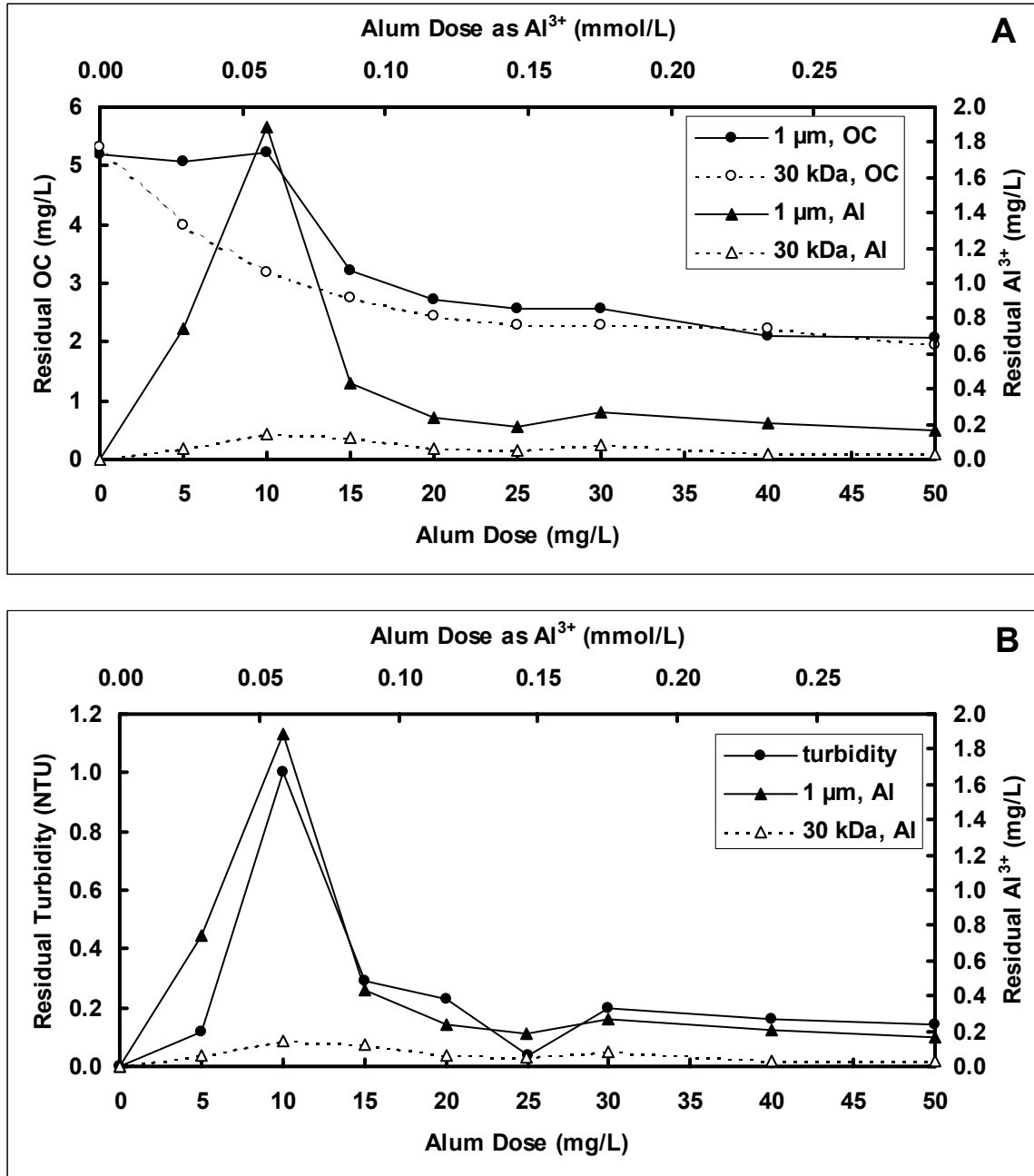


Figure 4. Phase separation of OC (panel A) and residual turbidity (panel B) in relation to coagulant dose. Nominal test water conditions were pH 6.8, 5 mg/L OC, 0 NTU turbidity (no added bentonite clay), and 25 °C. Filled symbols indicate material passing through 1 μm GF filter, open symbols indicate material passing through 30 kDa UF membrane.

the residual dissolved NOM fraction at all coagulant doses. The results indicate that much of the aluminum added ended up being incorporated into colloidal size particles. Further, these colloidal particles had a significant amount of NOM incorporated in some manner. The techniques used in this study could not define the specific mechanisms by which NOM removal was occurring. However, the work of Edzwald (1993) would suggest that NOM removal by alum under these conditions would be predominately by adsorption of NOM to the aluminum hydroxide colloids.

Coagulant metal was predominately segregated in the colloidal size range. As coagulant dose approached the terminal colloid dose, both colloidal aluminum and turbidity lines decreased dramatically. At coagulant doses above the colloidal dose range, the additional alum is hypothesized to have promoted aggregation on the NOM-containing aluminum hydroxide colloids to form particles of sufficient size to settle. Whatever mechanism was responsible for the formation of colloids in these jar tests, it is important to determine colloidal aggregate make-up. Characterization of colloids formed at sub-optimal coagulant doses may aid in selection of appropriate polymeric flocculant aids to enhance separation on NOM-coagulant aggregates by either settling or direct filtration.

3.2 Effect of pH on Colloid Formation

Test water pH had a large impact on the phase separation of NOM during coagulation. The colloidal regions formed during coagulation with alum were much larger for waters coagulated at pH 6.8 than at pH 5.8, as indicated in Figures 5 and 6. The increase in colloidal envelope area with pH was largely due to a pronounced shift in the envelope shoulders to higher coagulant doses at the higher pH. Furthermore, increased formation of colloidal OC was observed at pH 6.8 for each OC_0 level over the range of coagulant doses studied. The minimum residual OC level was lower at pH 5.8 than pH 6.8 for each OC_0 concentration examined, consistent with the pH range (5.5-6.0) of optimal OC removal using alum (Carlson and Gregory, 2000).

Data presented in Figure 7 show the corresponding residual turbidity results for pH 5.8 and 6.8, respectively. With the exception of the lowest OC_0 concentration at pH

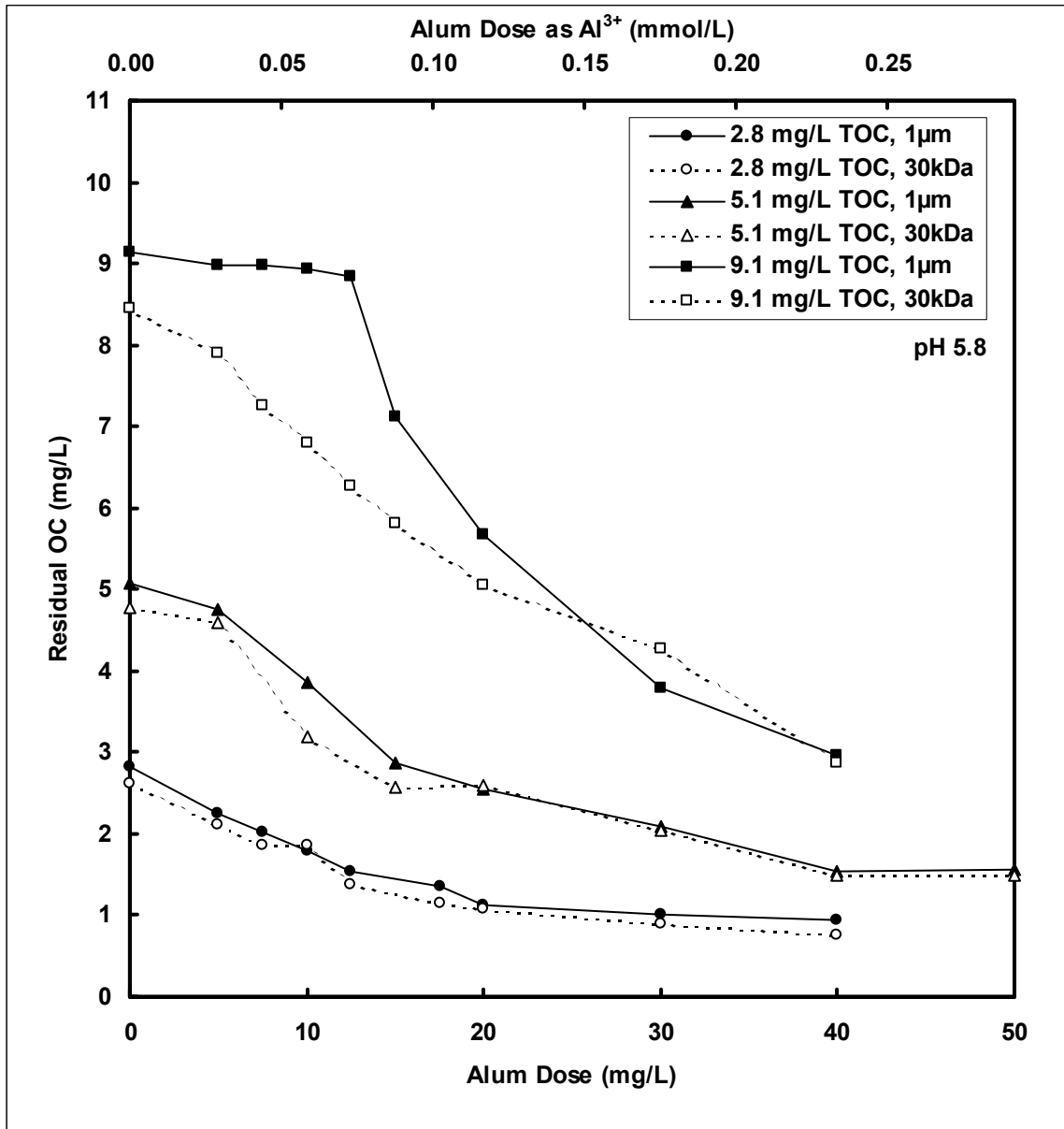


Figure 5. Organic carbon phase separation as a function of alum dose. Nominal test water conditions were pH 5.8, 10 NTU turbidity (bentonite clay), and 25 °C. Test water TOC as indicated in legend. Filled symbols indicate OC passing through 1 μ m GF filter, open symbols indicate OC passing 30 kDa UF membrane.

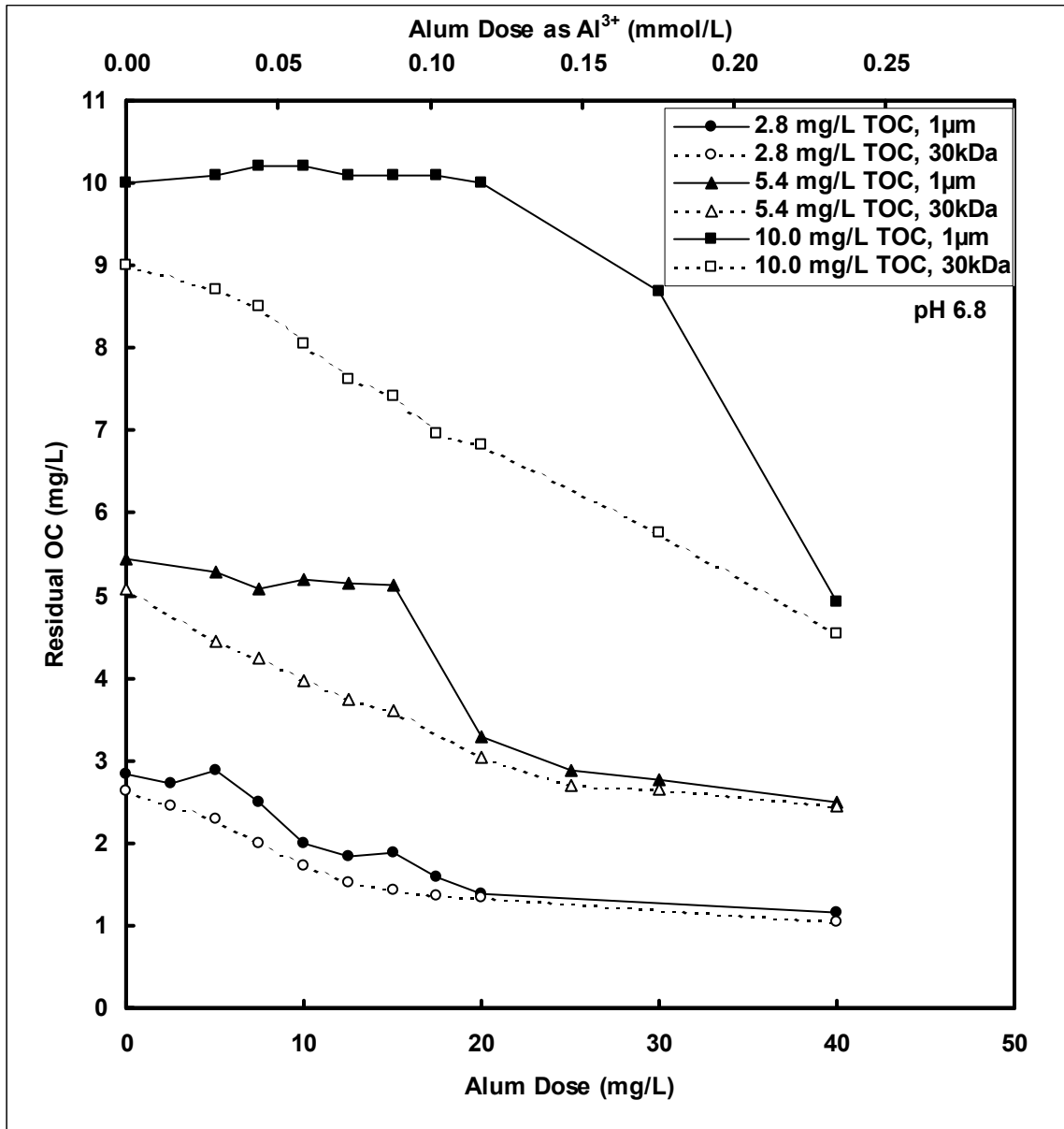


Figure 6. Organic carbon phase separation as a function of alum dose. Nominal test water conditions were pH 6.8, 10 NTU turbidity (bentonite clay), and 25 °C. Test water TOC as indicated in legend. Filled symbols indicate OC passing through 1 μ m GF filter, open symbols indicate OC passing through 30 kDa UF membrane.

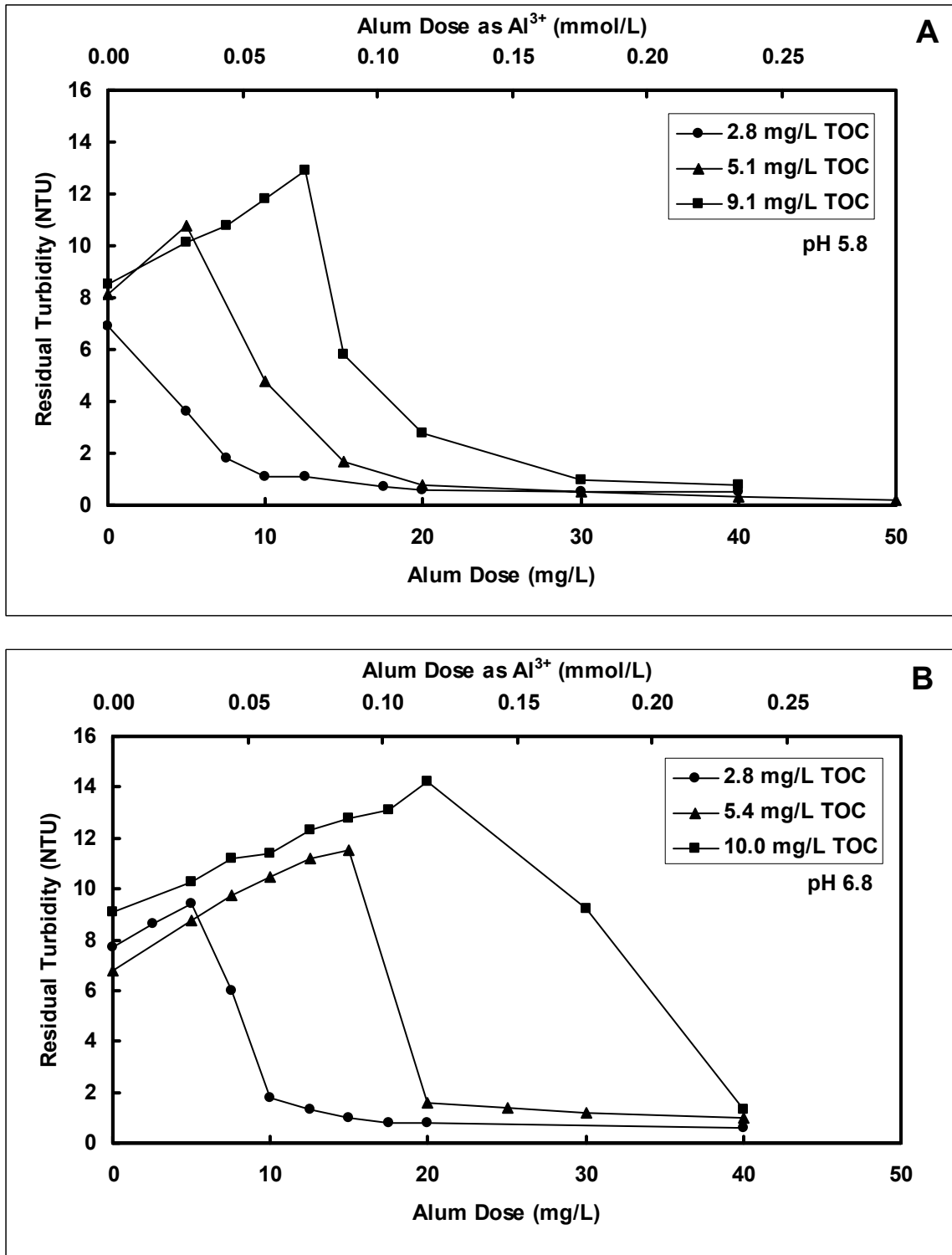


Figure 7. Residual turbidity as a function of alum dose. Nominal test water conditions were pH 5.8 (panel A), pH 6.8 (panel B), 10 NTU turbidity (bentonite clay), and 25 °C. Test water OC_0 as indicated in legend. envelope shoulders occurred at approximately the same normalized alum dose.

5.8, turbidity initially increased with alum dose, peaked at the coagulant dose corresponding to the maximum colloidal fraction, then decreased to low levels (< 1 NTU) with further coagulant addition. In each instance, the peak turbidity and shoulder of the OC colloidal region occurred at the particulate breakpoint dose (Figure 5 and Figure 6). Collectively, the residual OC and residual turbidity at both pH values indicate a similar pattern of OC phase separation in which soluble NOM and aluminum are incorporated in colloidal aggregates at low alum doses, with transition to the particulate phase at higher alum doses.

3.3 Effect of NOM Concentration on Colloid Formation

Test water NOM concentration strongly influenced OC phase separation during alum coagulation. The colloidal dose range and the maximum colloidal fraction increased with increasing test water OC_0 level, as shown in Figure 6. Residual turbidity was also significantly impacted by OC_0 , as the maximum residual turbidity and the corresponding particulate breakpoint dose both increased with OC_0 , as illustrated in Figure 7. Organic carbon phase separation and residual turbidity were intimately interrelated over the entire alum dose range. For each OC_0 examined, the particulate breakpoint dose (envelope shoulder) and the maximum residual turbidity coincided (compare data shown in Figures 6 and 7). At alum doses below the colloidal-particulate breakpoint, the colloidal fraction and residual turbidity increased concurrently, indicating incorporation of soluble OC in colloidal NOM-coagulant aggregates was the predominant phase separation process. The colloidal fraction and residual turbidity decreased rapidly in lock-step fashion at alum doses above the colloidal-particulate breakpoint, suggesting that flocculation of colloids to form settleable particles may be involved in formation of particulate OC.

Coagulant performance was compared for varying test water OC_0 values by normalizing OC phase separation (Figure 6) with respect to OC_0 in order to scale out the effects of varying OC_0 . When normalized by OC_0 , OC phase separation was essentially constant, showing only minor variation with OC_0 level, as shown in Figure 8. The envelope shoulders occurred at approximately the same normalized alum dose. A slight trend in OC phase separation of soluble NOM into the colloidal size fraction was

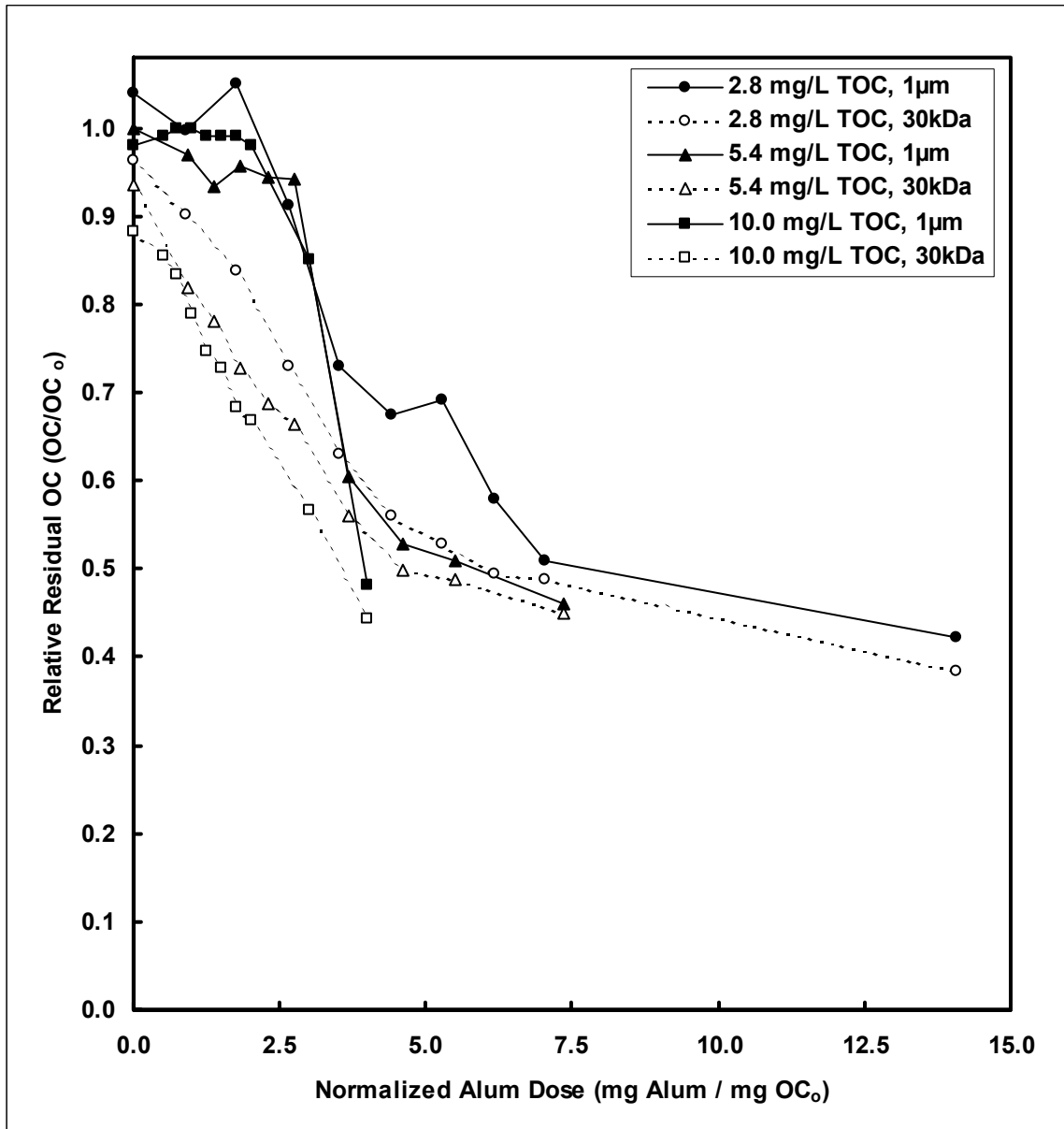


Figure 8. Normalized phase separation of OC as a function of alum dose. Nominal test water conditions were pH 6.8, 10 NTU turbidity (bentonite clay), and 25 °C. Test water OC₀ as indicated in legend (TOC). Filled symbols indicate OC passing through 1µm GF filter, open symbols indicate OC passing through 30 kDa UF membrane.

observed, as normalized residual OC passing a 30 kDa UF membrane decreased slightly with increasing OC_0 . This phenomenon may be related to the increased incorporation of soluble OC in NOM-Al-hydroxide colloids with increasing OC_0 (see colloidal fractions in Figure 6) as an equilibrium was established between the amount of OC in solution and the amount adsorbed on to colloids, rather than a fundamental difference in the mechanism(s) of soluble OC incorporation in these colloids.

Residual turbidity data were consistent with normalized OC phase separation. Although the maximum residual turbidity increased with increasing OC_0 , the normalized alum dose at peak residual turbidity was invariant, as illustrated in Figure 9. The normalized alum dose at peak residual turbidity also coincided with the shoulders of the normalized colloidal envelopes, indicating that a proportional increase in OC_0 required a proportional increase in coagulant to achieve the same level of OC phase separation. Collectively, the normalized OC separation and residual turbidity data shown in Figure 8 and Figure 9 provides evidence that the mechanism(s) that control NOM incorporation in colloidal aggregates were only minimally affected if at all by OC_0 level.

3.4 Effect of Initial Turbidity on Colloid Formation

The presence of bentonite clay affected colloid formation behavior as demonstrated by a decrease in the colloidal fraction with increasing initial turbidity (as shown by data contained in Figure 10). This decrease in the colloidal fraction was predominantly due to less phase separation of OC from dissolved into colloidal matter with increasing initial turbidity, as shown by the 30 kDa UF data. The envelope shoulder shifted towards the same higher alum dose in tests with added turbidity (9.2 NTU and 23.2 NTU). The turbidity data peaks also shifted to the same higher alum dose, coinciding with the respective envelope shoulder (Figure 11).

NOM concentration is generally thought to control optimum coagulant dose for OC removal, although the results from varying bentonite concentration suggest that turbidity exerted some coagulant demand on the system. Because the results from jar tests with varying turbidity indicated that some alum interacted with the bentonite, more alum was required to complete NOM phase-shift from colloidal to particulate matter in

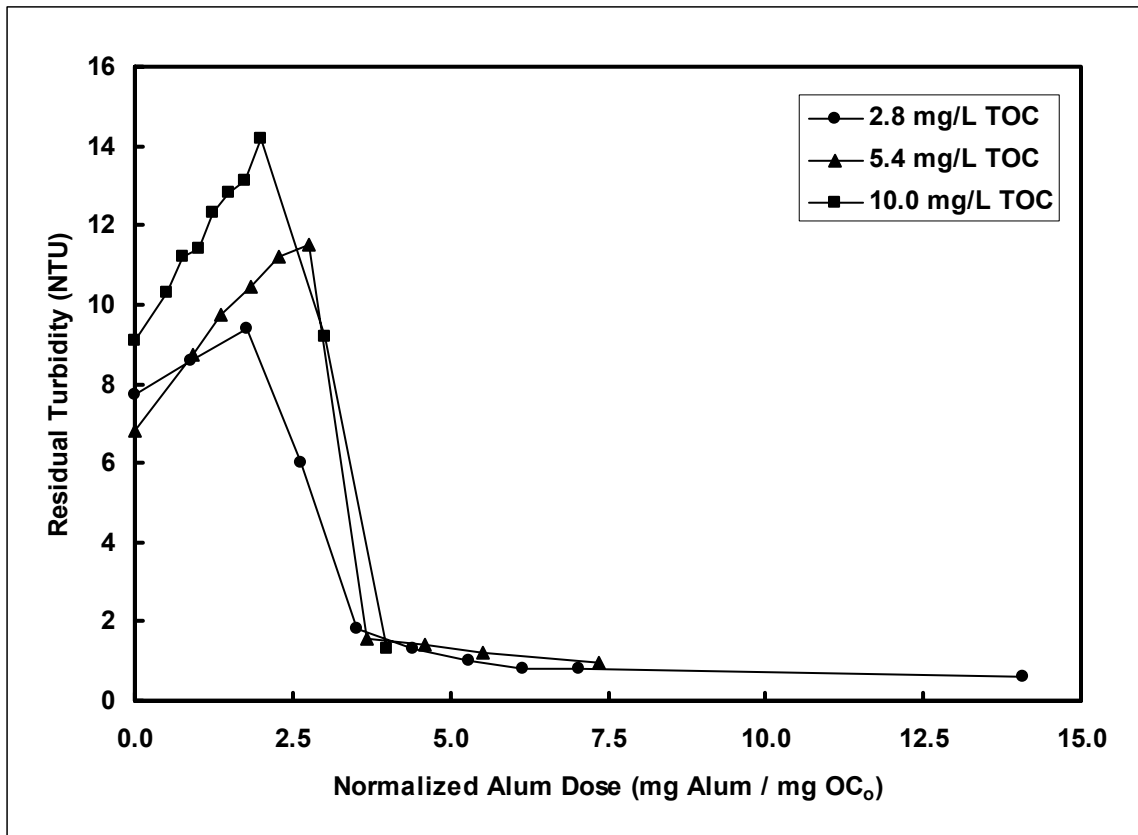


Figure 9. Residual turbidity as a function of alum dose. Horizontal axis normalized with respect to initial OC concentration. Nominal test water conditions were pH 6.8, 10 NTU turbidity (bentonite clay), and 25 °C. Test water OC₀ as indicated in legend (TOC).

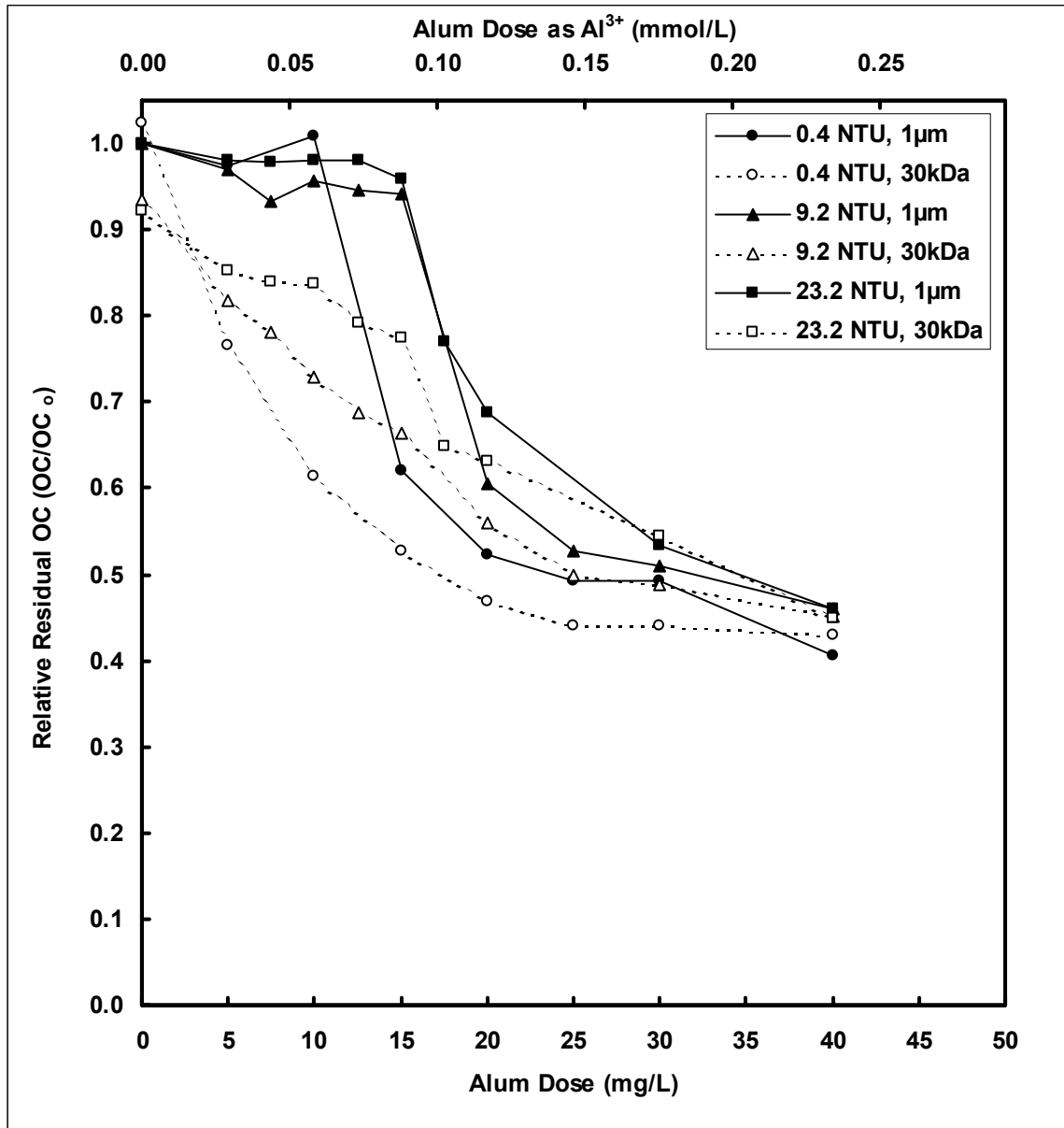


Figure 10. Organic carbon phase separation as a function of alum dose. Vertical axis normalized with respect to initial test water OC concentration. Nominal test water conditions were pH 6.8, 5 mg/L OC, and 25 °C. Test water turbidity as indicated in legend. Filled symbols indicate OC passing through 1 μm GF filter, open symbols indicate OC passing through 30 kDa UF membrane.

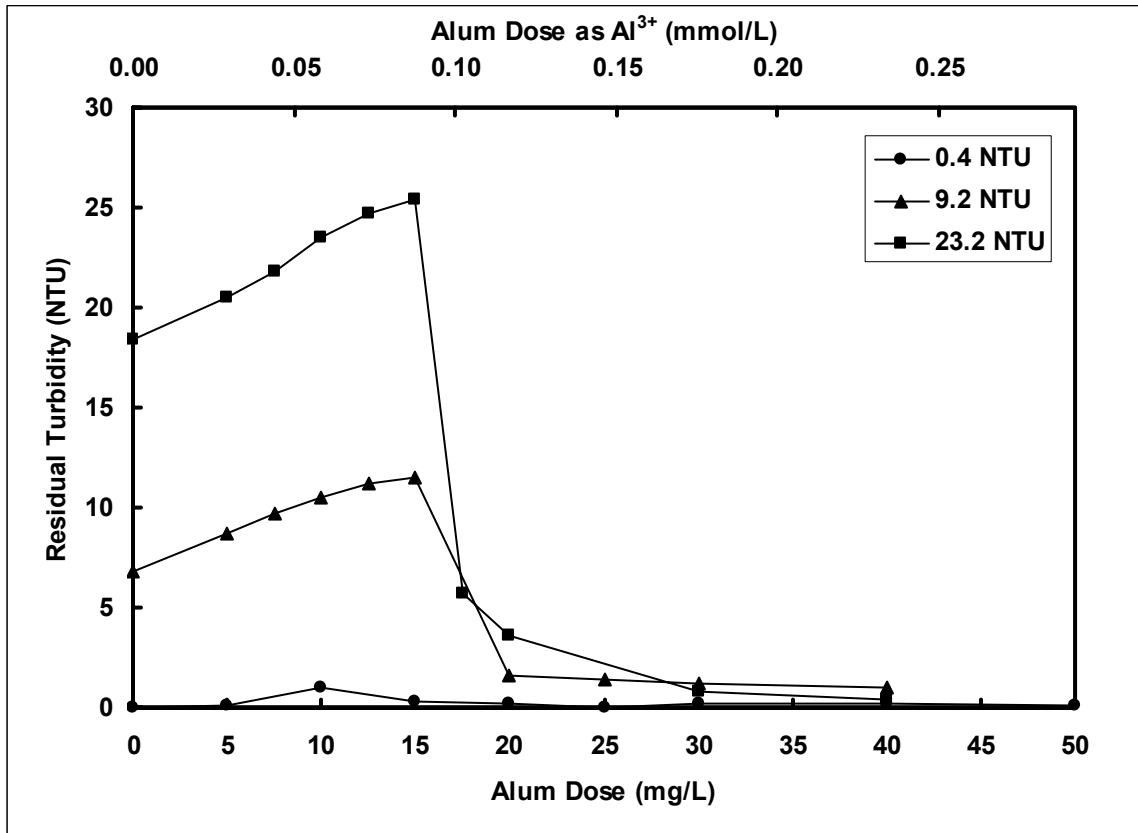


Figure 11. Residual turbidity as a function of coagulant dose. Nominal test water conditions were pH 6.8, 5 mg/L OC, and 25 °C. Test water turbidity as indicated in legend.

the presence of bentonite. Furthermore, the decrease in the colloidal fraction revealed that less NOM was associated with colloids as the amount of turbidity increased (Figure 10). The overall effect is that some competition was present between NOM and bentonite for the aluminum added during coagulation, however, the normalized OC phase separation and residual turbidity data suggest that OC_o largely controlled coagulant demand, which is consistent with the published work of Bose and Reckhow (1998) and Edzwald (1993).

3.5 Effect of Coagulation Temperature on Colloid Formation

Coagulation temperature had an effect on particulate matter formation as the particulate breakpoint dose was increased at 4 °C for all three OC_o values studied, as shown in Figures 12-14, panel A. Turbidity data supported this shift in particulate matter formation as the turbidity peak at 4 °C also occurred at a higher alum dose corresponding with the envelope shoulder (Figures 12-14, panel B). An exception was noted for 5 mg/L OC_o where the turbidity peaks occurred at the same alum dose (Figure 13, panel B). Similar behavior of a shift in particulate matter formation to a higher alum dose was still observed as the turbidity at 4 °C approached 0 NTU at a higher alum dose, which corresponded with the terminal colloidal dose in Figure 13, panel A. The level of NOM removal was similar at both coagulation temperatures studied over the entire dose range as demonstrated by the congruence of the 30 kDa OC filtration behavior at both temperatures. There was a slight effect of temperature on settling observed in the control jars with no added alum (Figures 13 and 14, panel B). While the difference in initial versus residual turbidity was similar in the control jars with 2.5 mg/L OC_o , the difference in initial versus residual turbidity was greater at 25 °C with both 5 mg/L and 10 mg/L OC_o ,

Collectively, these observations suggest that there was an effect of temperature on floc formation, with floc formation performance decreasing at 4 °C. While there was little effect of temperature on OC phase separation from a dissolved state to a suspended state, there was however, an effect on the formation of particulate matter. This suggests that temperature affected the ability of the formed colloids to aggregate into particles of sufficient size to settle out of solution or be retained by a 1 μ m GF filter. One possible explanation is that flocculation kinetics may have decreased with temperature due to

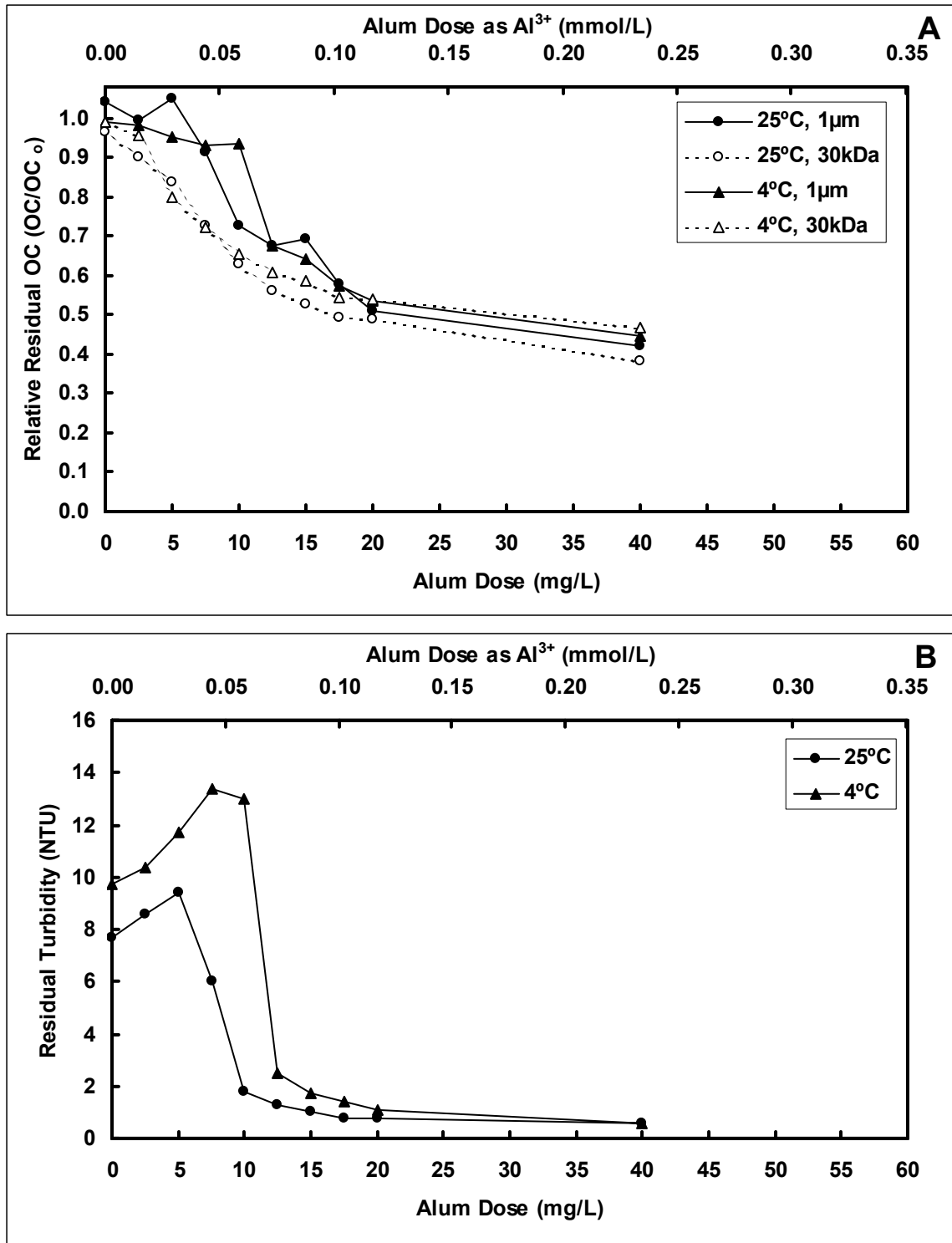


Figure 12. Panel A – residual OC as a function of coagulant dose. Vertical axis normalized with respect to OC₀. Panel B – residual turbidity as a function of coagulant dose. Nominal test water OC₀ was 2.5 mg/L. Circles indicate 25 ° C, pH 6.8, test water turbidity was 8.1 NTU. Triangles indicate 4 ° C, pH 7.5, test water turbidity was 10.1 NTU.

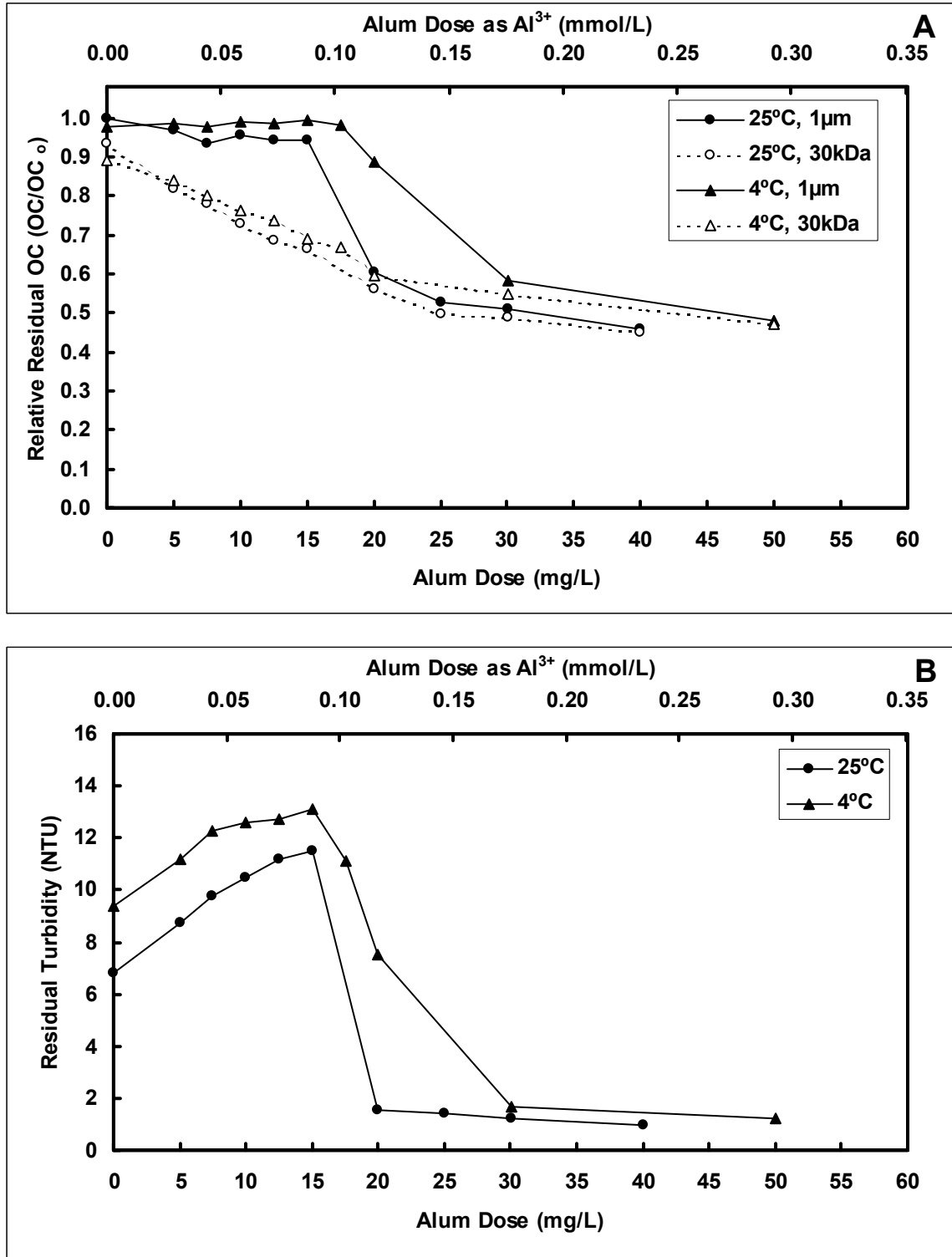


Figure 13. Panel A – residual OC as a function of coagulant dose. Vertical axis normalized with respect to OC₀. Panel B – residual turbidity as a function of coagulant dose. Nominal test water OC₀ was 5 mg/L. Circles indicate 25 °C, pH 6.8, test water turbidity was 9.2 NTU. Triangles indicate 4 °C, pH 7.5, test water turbidity was 9.9 NTU.

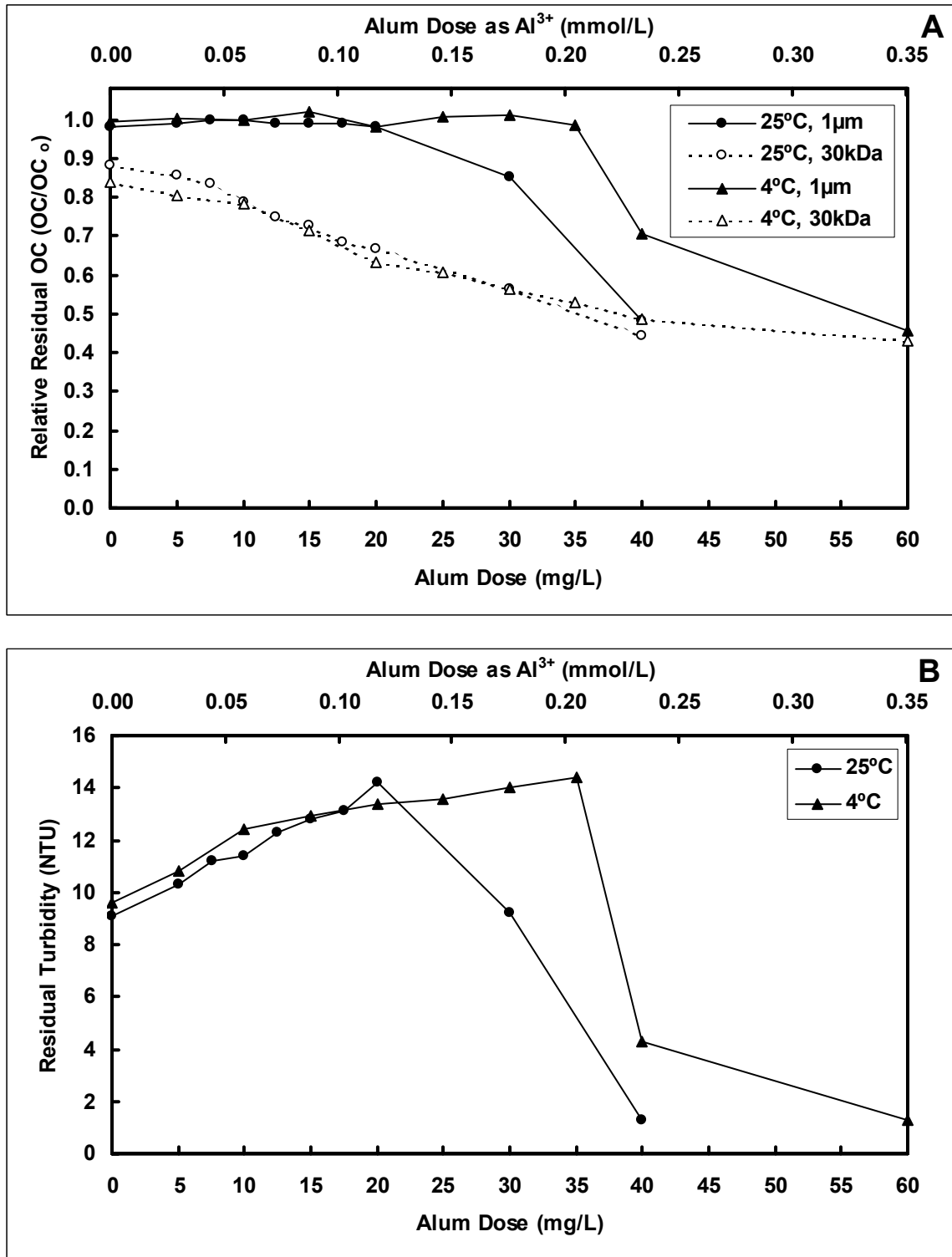


Figure 14. Panel A – residual OC as a function of coagulant dose. Vertical axis normalized with respect to OC₀. Panel B – residual turbidity as a function of coagulant dose. Nominal test water OC₀ was 10 mg/L. Circles indicate 25 °C, pH 6.8, test water turbidity was 10.1 NTU. Triangles indicate 4 °C, pH 7.5, test water turbidity was 9.5 NTU.

higher water viscosity at 4 °C. Under the same mixing conditions (paddle rotation speed and time) the formation of large floc was inhibited by a colder, more viscous solution. As a result, more coagulant was required to achieve the particulate breakpoint dose at the colder temperatures studied. The differences in initial versus residual turbidity observed in the control jars can be explained by Stokes Law, which demonstrates that particles of the same size and density settle slower at lower solution temperatures due to higher viscosity. Initial turbidity was added using bentonite clay and these results suggest that bentonite settling rates were affected by solution temperature.

As discussed previously, both OC_0 and initial turbidity affected colloid formation. These effects were ruled out as playing a role in the temperature trends. The vertical axes were normalized with respect to OC_0 to negate any differences in OC_0 between the two tests compared in each plot. With regards to the initial turbidity, only the low OC_0 test in Figure 12 had a notable difference in initial turbidity. The medium and high OC_0 tests had similar initial turbidities, with the cold test being higher in Figure 13 and lower in Figure 14. The discussed trends shown in the results occurred irrespective of these differences.

3.6 Characterization of Colloid Zeta Potential as a Result of Coagulation

Zeta potential data were inconclusive in attempting to characterize the charge associated with the NOM-aluminum hydroxide colloidal aggregates formed during alum coagulation. The average zeta potential did not change substantially with jar test stage in either experiment with added NOM, as shown in Table 3. The water samples coagulated with 12.5 mg/L alum were representative of conditions favorable for phase separation of dissolved NOM into colloidal matter but not into particulate matter (see Figure 6, 5.4 mg/L OC_0). The water samples coagulated with 20 mg/L alum that contained OC_0 were representative of conditions favorable for phase separation of dissolved NOM into particulate matter (see Figure 6, 5.4 mg/L OC_0). In the absence of NOM, average zeta potential became substantially less negative within the first minute of coagulation and remained steady in all subsequent jar test stages (Table 3, nominal test water turbidity was 10 NTU, residual turbidity was 0.5 NTU).

Table 3. Average zeta potential as a function of jar test stage, alum dose, and test water OC_0 concentration as noted in table. Nominal test water conditions were pH 6.8, 10 NTU turbidity, and 25 °C. Average was taken from five readings of each sample.

Test Water		Average Zeta Potential (mV)						
Alum Dose (mg/L)	OC_0 (mg/L)	Untreated	Coagulation (1 min.)	Coagulated	1st Stage Flocculation (5 min.)	2nd Stage Flocculation (5 min.)	Flocculated	Settled
12.5	4.8	-37.1	---	-37.3	---	---	-36.7	-37.7
20.0	4.0	-37.9	-35.9	-35.3	-34.9	-35.6	-36.1	-37.0
20.0	0.0	-35.3	-22.9	-22.8	-23.5	-24.1	-24.2	-24.6

One possible explanation for inconclusive zeta potential results with respect to NOM associated colloidal matter is that the aggregates were sheared either during sample acquisition or injection into the zeta potential instrument using a syringe, or electrophoretic motion in the instrument capillary tube. Both steps of this process involved forcing the sample through very narrow orifices. The resulting increased velocity may have sheared the aggregates formed during coagulation. It is undetermined whether the NOM-coagulant metal-clay aggregates are tightly bound or loosely associated; however, shearing may have occurred if the latter was the case. Zeta potential results in the absence of NOM may have demonstrated a charge effect because the coagulant metal-clay aggregates were more tightly bound and stable enough to withstand the shearing forces subjecting during the sampling/analysis process, or the absence of negatively charged NOM resulted in more positively charged coagulant metal-clay aggregates.

3.7 Optimization of NOM Removal Using Polymeric Flocculant Aids

The results presented in this study consistently demonstrated the occurrence of OC phase separation during alum coagulation. Phase separation was characterized by the formation of OC associated colloidal matter at low alum doses, then transitioning into particulate matter as the alum dose was increased beyond the particulate breakpoint dose. With inorganic coagulants such as alum, typical treatment strategies employed for D/DBP Rule compliance dictate that plants operate at coagulant doses sufficient for good particulate matter formation. The objective of these polymer experiments was to evaluate the potential for replacing a large amount of the alum with low doses of polymeric flocculant aids, whereby using the polymers to further aggregate colloidal matter formed at low alum dose conditions. This was attempted by adding selected polymers during either first- or third-stage flocculation following alum coagulation (see section 2.3). All jar tests incorporating polymers were coagulated with 15 mg/L alum, which was representative of conditions favorable for phase separation of dissolved NOM into colloidal matter but not into particulate matter (i.e. below particulate breakpoint dose; see Figure 5, 10 mg/L OC₀).

Polymeric flocculant aids chosen for this research did not demonstrate further phase separation behavior from colloidal to particulate matter following low alum dose coagulation. The amount of OC associated colloidal matter formed during alum coagulation was fairly constant throughout the polymer dose range for all polymers studied, as shown by the similar separation in 1 μ m and 30 kDa filtration data (Figure 15). Turbidity increased from the test water value due to colloidal matter formed by alum, and remained fairly unchanged with increasing polymer dose (Figure 16). One exception was noted in the experiment conducted with the 250,000 amu cationic polymer (Superfloc C-581) in which turbidity increased during the first polymer dose, and then remained constant with all subsequent polymer doses.

Previous work demonstrated phase separation of colloidal to particulate matter resulting from polymeric flocculant aid addition following low alum dose coagulation (Siczka, 1997). There were some differences in coagulation experimental parameters that existed between Siczka's work and this research, and are summarized in Table 4. These results from the previous work showed that colloidal matter decreased with increasing polymer dose until no colloidal matter remained at a dose of 0.3 mg/L, then increased to the original value at subsequently higher polymer doses, and dissolved NOM remained constant throughout the polymer dose range. An unsuccessful attempt was made in this research to demonstrate the same phenomenon seen in Siczka's work using the same polymer (Ondeo Nalco Pol-E-Z® 652), with additional polymers included in this study. The following differences may have been responsible for incongruent results between previous and present work: NOM source (Lake Drummond <10 kDa hydrophobic acid fraction versus Suwannee River <30 kDa unfractionated), pH (5.8 versus 6.8), and turbidity (no added turbidity versus 10 NTU). Further investigation into the charge and structure of the colloidal matter formed during alum coagulation may aid in the selection of an appropriate polymer.

3.8 Comparison of Colloid Formation Between Alum and Iron Sulfate

The bulk of this research presented OC phase separation resulting from alum coagulation, chosen for its wide use by water treatment utilities. However, ferric iron is another trivalent cation that is widely employed as a primary coagulant metal in water

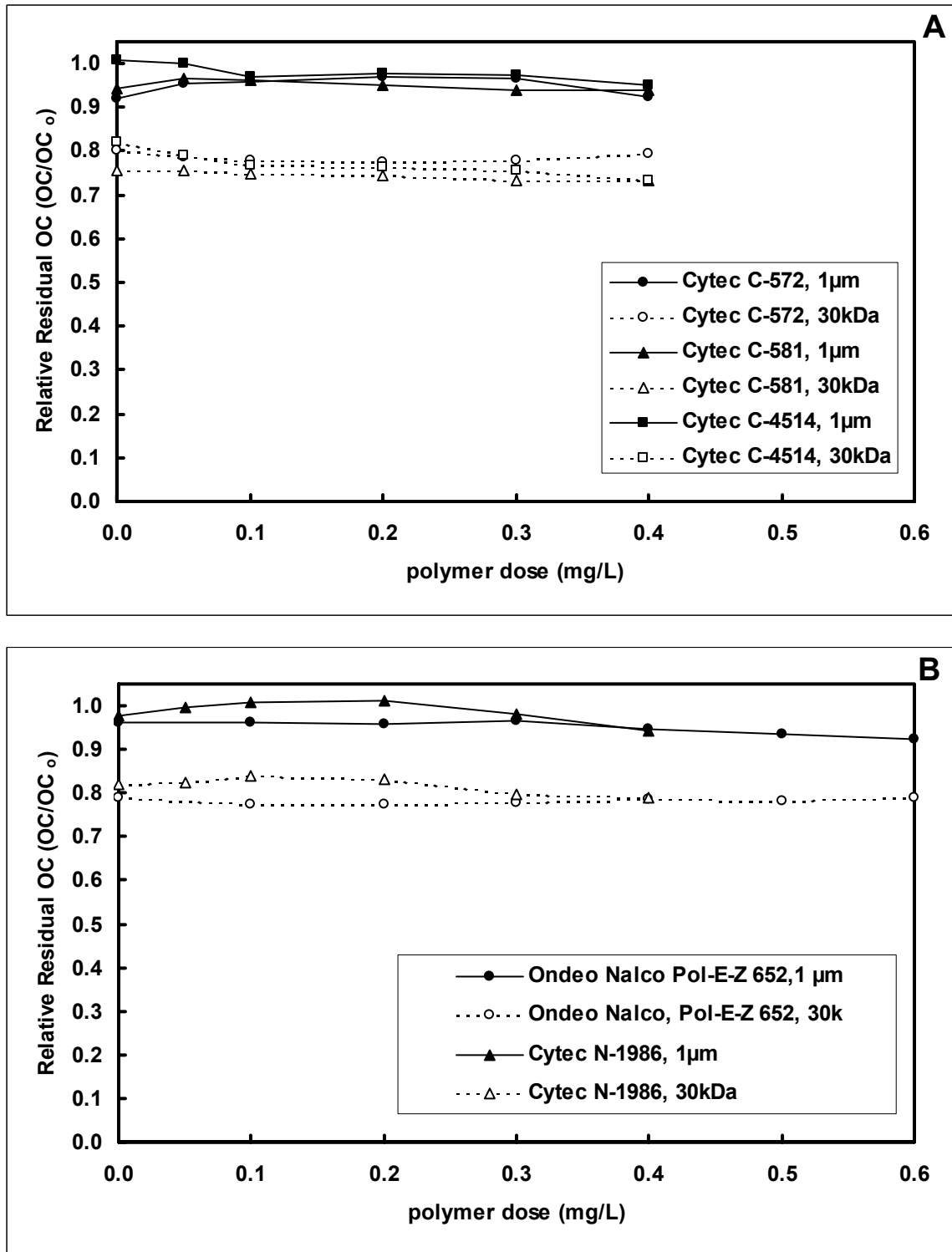


Figure 15. OC phase separation as a function of polymer dose. Panel A – cationic polymers with varying nominal molecular weight (see Table 2). Panel B – nonionic polymers with similar molecular weight (see Table 2). Nominal test water conditions were pH 6.8, 10 mg/L OC₀, 10 NTU turbidity, and 25 °C.

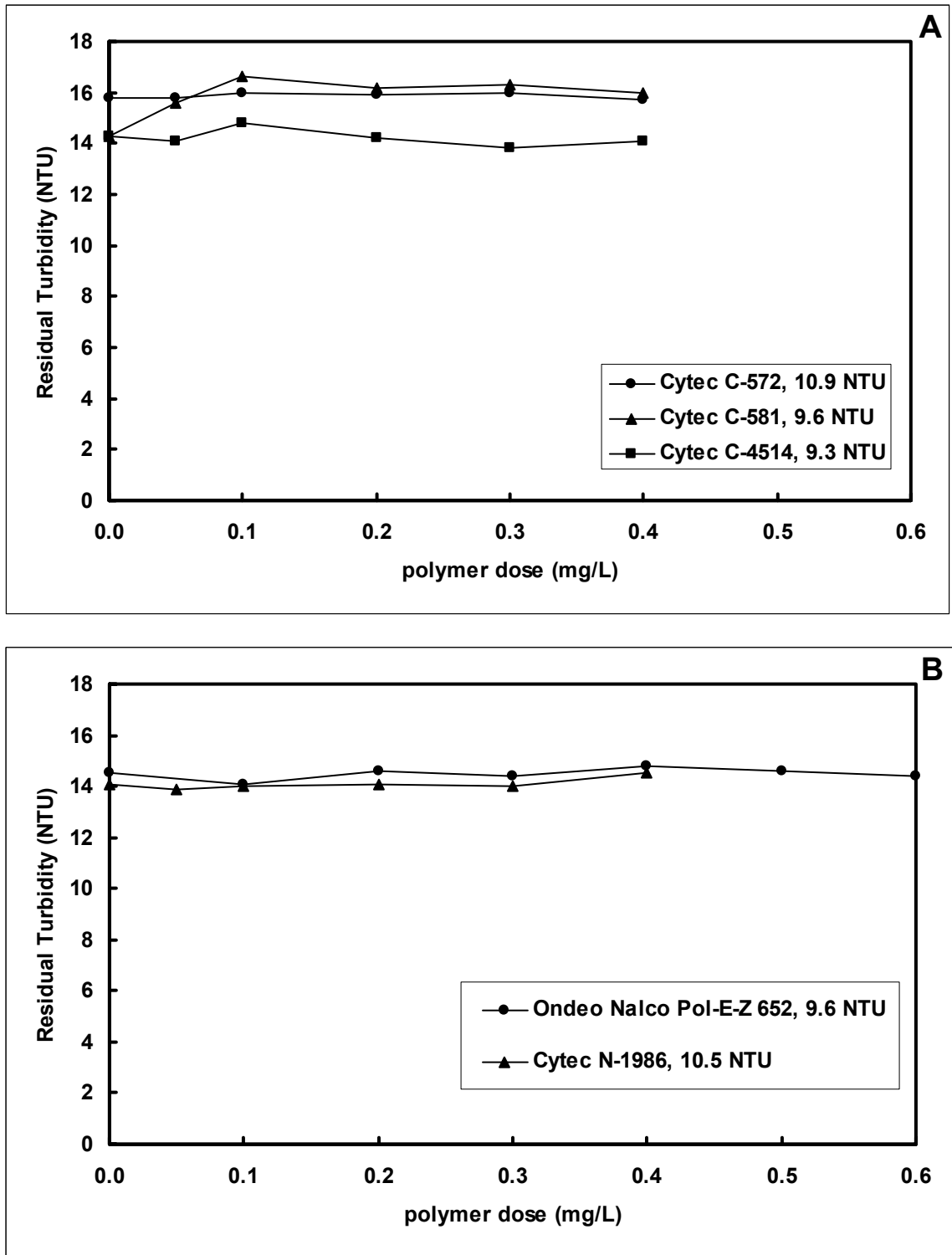


Figure 16. Residual turbidity as a function of polymer dose. Panel A – cationic polymers with varying nominal molecular weight (see Table 2). Panel B – nonionic polymers with similar molecular weight (see Table 2). Nominal test water conditions were pH 6.8, 10 mg/L OC_o , and 25 °C. Test water turbidity as shown in legend.

Table 4. Differences in experimental conditions between this research and previous work (Siczka, 1997) in demonstration of polymers to enhance OC phase separation from colloidal to particulate matter. Refer to Table 2 for further details of polymer types.

	Previous Work	This Research
NOM type	< 10 kDa hydrophobic acid fraction, Lake Drummond, VA	< 30 kDa non-fractionated, Suwannee River, FL
initial OC ₀	5 mg/L	10 mg/L
alum dose	12.5 mg/L	15 mg/L
GF filter	1 μm	1 μm
UF membrane	100 kDa	30 kDa
polymer dose stage	1st stage flocculation	1st and 3rd stage flocculation
polymer type	Pol-E-Z 652	Pol-E-Z 652 and Cytac

treatment. As a result, alum and iron sulfate were compared on an equivalent (molar) basis in terms of OC phase separation and residual turbidity response.

Transition from colloidal to particulate matter formation occurred at a lower aluminum dose when compared to ferric iron on a molar basis for all test water conditions examined (iron sulfate data from previous study, Masters, 2003). Aluminum had a lower particulate breakpoint dose than ferric iron signified by a shift in the envelope shoulder (shown in panel A of Figures 17-20). The amount of NOM removal in terms of incorporation of OC into colloidal aggregates was similar for both aluminum and ferric iron demonstrated by the congruence of the 30 kDa filtration data. Residual turbidity after settling initially increased with a similar slope for both coagulant metals, giving further evidence that colloid formation behavior was similar as a function of coagulant dose (Figures 17-20, panel B). Maximum residual turbidity occurred at a coagulant dose coinciding with the particulate breakpoint dose throughout this investigation of OC phase separation, regardless of coagulant or test water conditions.

Overall, the OC phase separation behavior coinciding with the residual turbidity response for alum and iron sulfate was consistently observed. Formation of the colloidal region at low coagulant doses was observed for both coagulants, with transitioning into particulate matter at higher coagulant doses. Likewise, residual turbidity increased with increasing colloid formation up to some critical coagulant dose, peaked, and then decreased rapidly.

There is an apparent difference in behavior between aluminum and iron that should be noted. For average source waters, aluminum has been reported to form complexes with NOM at a ratio of approximately 0.6 mg Al/mg OC (Edzwald, 1993). Estimates for iron-NOM complexation ranged from 0.01 mg Fe/mg OC to 0.05 mg Fe/mg OC (Tadanier *et al.*, 1997). The difference between the two coagulant metals amounts to approximately 25 times more aluminum-NOM complexation as compared to iron on a molar basis. However, a review of the Edzwald (1993) study suggests that a significant portion of the organic material classified as “complexed” may have in fact been “colloidal” by the operational definition of the current study. Despite this important difference between the coagulant metals, these data were incomplete in terms of providing speculation into why the particulate breakpoint doses were different.

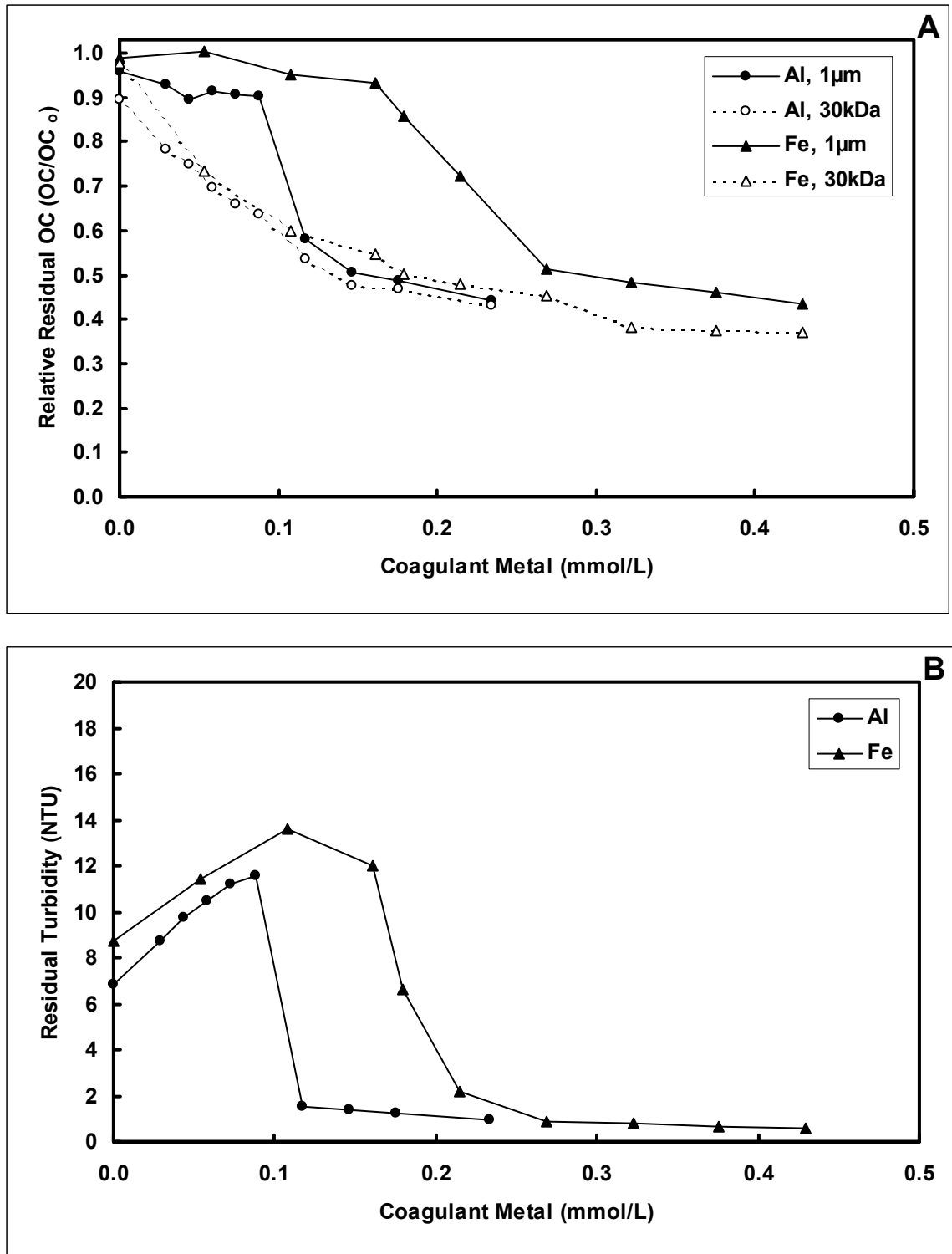


Figure 17. Comparison of alum and iron sulfate coagulant performance on a molar basis. Panel A - OC phase separation as a function of coagulant metal concentration, panel B - residual turbidity. Nominal test water conditions were 5 mg/L OC₀, pH 6.8, 10 NTU turbidity, and 25 °C. Circles indicate alum, triangles indicate iron sulfate.

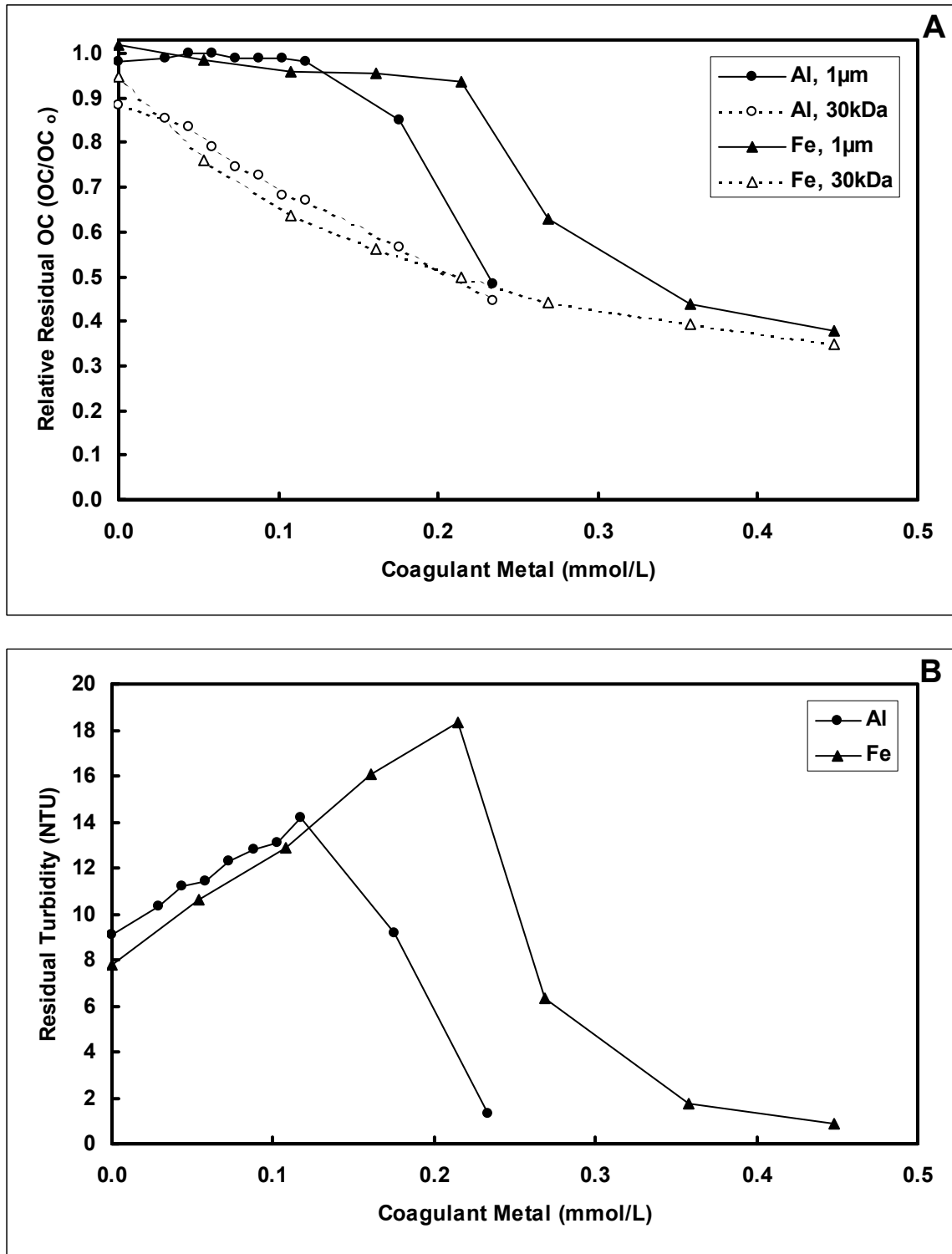


Figure 18. Comparison of alum and iron sulfate coagulant performance on a molar basis. Panel A - OC phase separation as a function of coagulant metal concentration, panel B - residual turbidity. Nominal test water conditions were 10 mg/L OC₀, pH 6.8, 10 NTU turbidity, and 25 °C. Circles indicate alum, triangles indicate iron sulfate.

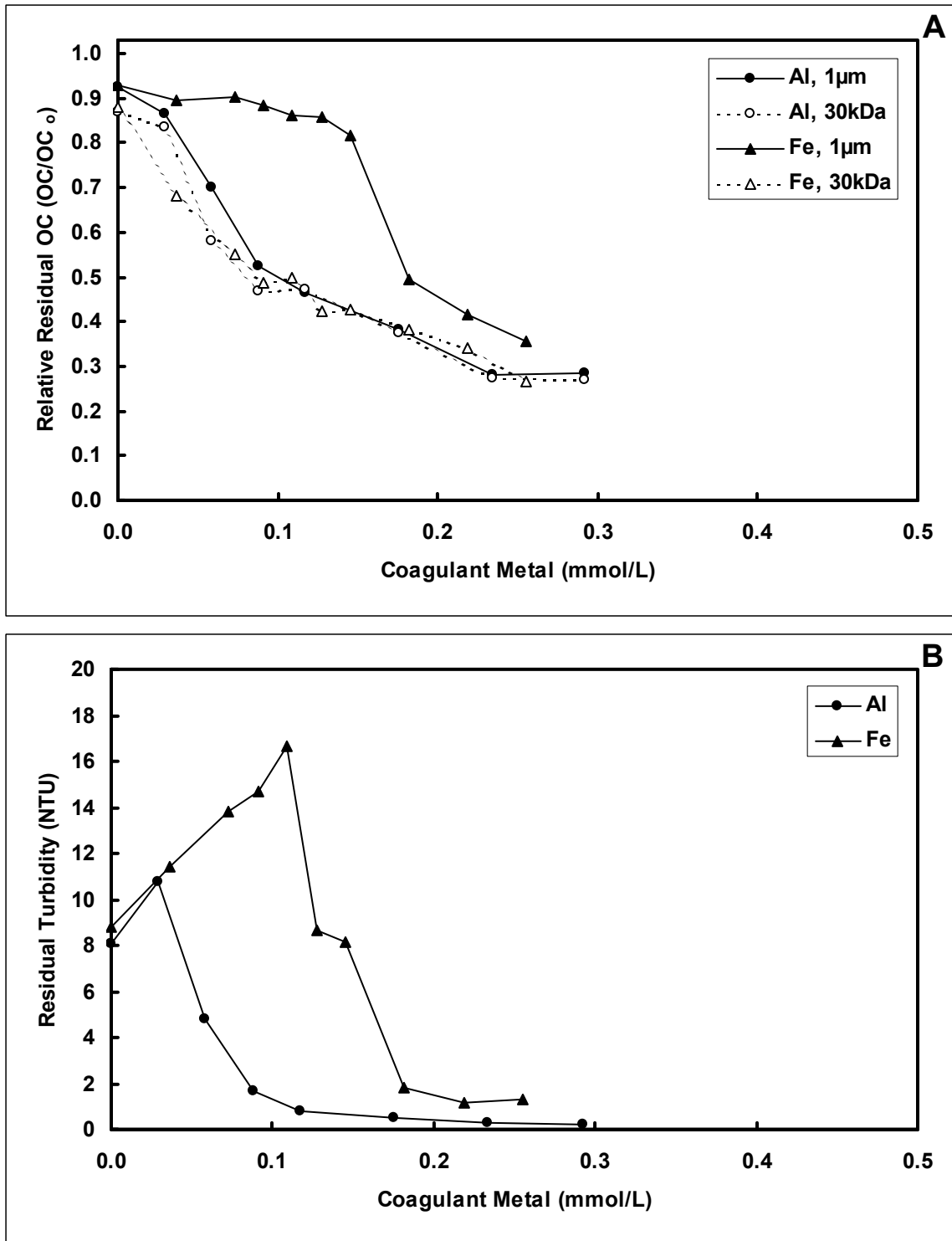


Figure 19. Comparison of alum and iron sulfate coagulant performance on a molar basis. Panel A - OC phase separation as a function of coagulant metal concentration, panel B - residual turbidity. Nominal test water conditions were 5 mg/L OCo, pH 5.8, 10 NTU turbidity, and 25 °C. Circles indicate alum, triangles indicate iron sulfate.

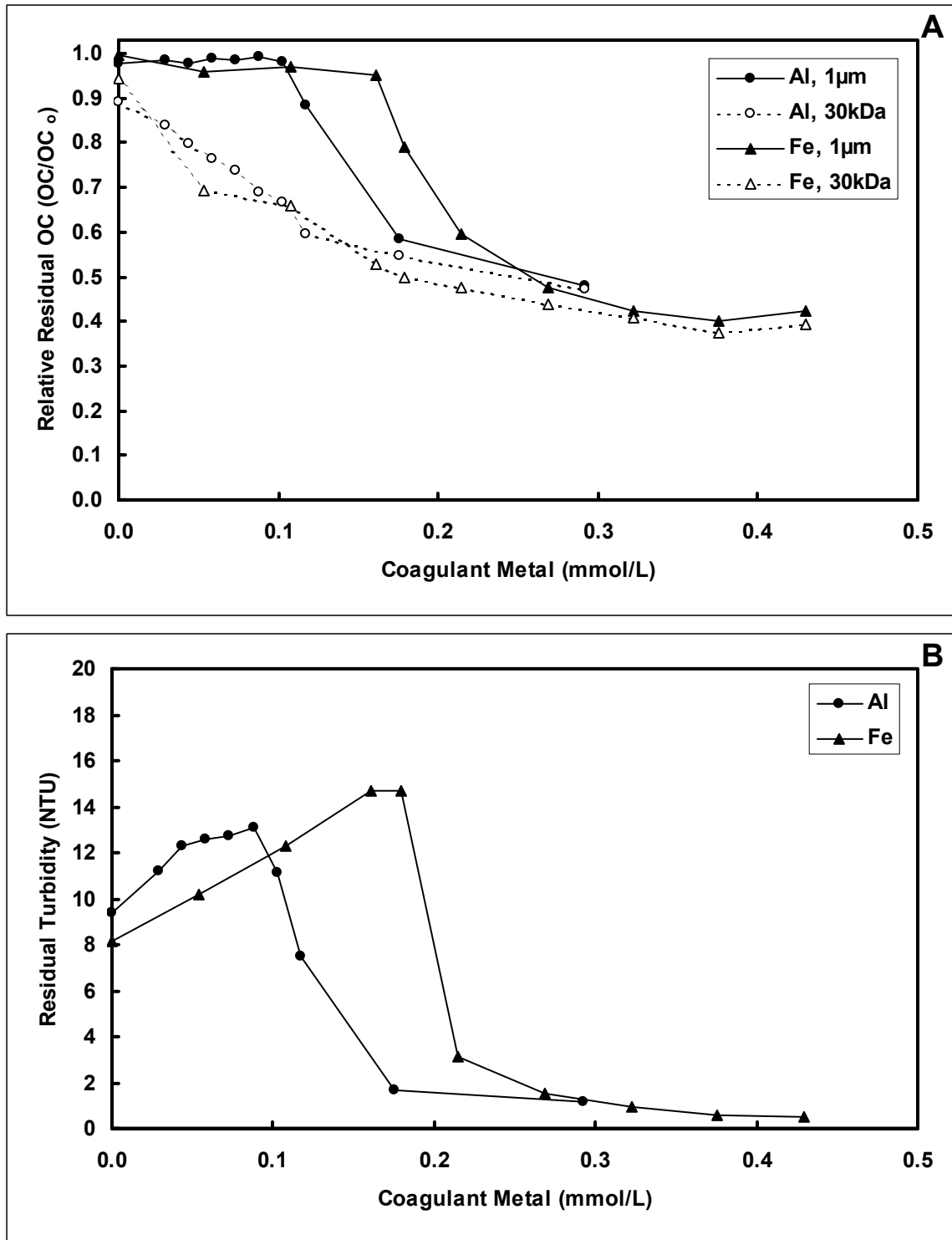


Figure 20. Comparison of alum and iron sulfate coagulant performance on a molar basis. Panel A - OC phase separation as a function of coagulant metal concentration, panel B - residual turbidity. Nominal test water conditions were 5 mg/L OC₀, pH 7.5, 10 NTU turbidity, and 4 °C. Circles indicate alum, triangles indicate iron sulfate.

Successful quantification of the charge and structure of formed colloidal matter may have provided valuable insight, and is suggested for further studies.

CHAPTER 4: CONCLUSIONS

This research accomplished three main objectives. First, OC phase separation into three size fractions (dissolved, colloidal, and particulate) resulting from alum coagulation was documented for varied test water conditions. The test water conditions examined were pH, NOM concentration, turbidity, and temperature. Second, the potential use of varied molecular weight cationic and anionic polymers as flocculant aids was investigated in an effort to demonstrate optimization of OC removal with respect to coagulant dose. Finally, the relative performance of alum and iron sulfate for OC phase separation was evaluated on a comparative molar metal basis.

Throughout this research, similar OC phase separation behavior was consistently shown to occur, whereby a colloidal region was formed at relatively low coagulant doses. The colloidal region was characterized by OC becoming incorporated into colloidal matter at low coagulant doses and transitioning into particulate matter at higher coagulant doses, operationally defined by 30 kDa UF membrane and 1 μ m GF filter cutoffs, respectively. The residual turbidity response was shown to relate directly to OC phase separation. Residual turbidity increased with increasing colloid formation as alum was added up to some critical dose (termed particulate breakpoint dose in this research), at which turbidity peaked. At alum doses just beyond the critical dose, a rapid increase in particulate matter formation was accompanied by a rapid decrease in residual turbidity. Likewise, residual colloidal aluminum increased rapidly, peaked at the same critical dose, and decreased rapidly beyond the critical dose.

Test water pH and initial NOM concentration both had a significant effect on OC phase separation. Regarding pH, a larger colloidal region was formed at pH 6.8 than at pH 5.8, signified by an increase in the dose at which particle formation first occurred at pH 6.8. Furthermore, better overall OC removal was observed at pH 5.8. Regarding initial NOM concentration, colloidal region increases in size with increasing NOM concentration. At alum doses within the colloidal region, the separation between the residual 1 μ m and 30 kDa OC data increased with increasing initial NOM concentration. Likewise, the dose at which particle formation first occurred increased with increasing initial NOM concentration. The increase in colloidal matter formation was shown to be

directly proportional to the increase in initial NOM concentration, which suggested that NOM concentration to a large degree controlled coagulant demand.

There was an effect of temperature on floc formation, with larger floc forming at lower alum doses during coagulation at 25 °C as compared to 4 °C. This was signified by the formation of particulate matter at a lower alum dose at 25 °C. . Temperature and initial turbidity both had a minor effect on OC phase separation from a dissolved state to a suspended state, as NOM removal by 30 kDa ultrafiltration was similar under compared coagulation conditions. Initial turbidity exerted some amount of coagulant demand, signified by a decrease in the separation between the residual 1µm and 30 kDa OC data with increasing initial turbidity.

The ability for low doses of polymers to replace a large portion of alum in order to further aggregate colloids was not demonstrated in this research. Polymer selection based on charge and size as well as the methodology of polymer addition to the jar tests may be critical in successful colloid aggregation. Further research is suggested.

Alum and iron sulfate were compared in terms of OC phase separation and residual turbidity response. When compared on a molar coagulant metal basis, the amount of OC associated with colloidal matter was similar, while the critical coagulant dose at which particulate matter formed was shifted to a much higher dose for iron. This resulted in the formation of colloids over a much larger dose range for iron as compared to aluminum. These comparisons were consistently observed over the entire range of test water conditions examined.

REFERENCES

- Bose, Purnendu, and David A. Reckhow (1998) "Adsorption of Natural Organic Matter on Preformed Aluminum Hydroxide Flocs." Journal of Environmental Engineering **124**(9): 803-811.
- Browne, B. A. and C. T. Driscoll (1993) "pH-Dependent Binding of Aluminum by a Fulvic Acid." Environmental Science and Technology **27**(5): 915-922.
- Carlson, Kenneth H. and Dean Gregory. (2000). "Optimizing Water Treatment with Two-Stage Coagulation." Journal of Environmental Engineering **126**(6): 556-561.
- Chaiket, Thom, Philip C. Singer, Amy Miles, Melissa Moran, and Catherine Pallotta. (2002) "Effectiveness of coagulation, ozonation, and biofiltration in controlling DBPs." Journal American Water Works Association **94**(12): 81-95.
- Crozes, Gil, Patrick White, and Matthew Marshall. (1995). "Enhanced coagulation: Its effect on NOM removal and chemical costs." Journal American Water Works Association **87**(1): 78-89.
- Edwards, Marc. (1997) "Predicting DOC removal during enhanced coagulation." Journal American Water Works Association **89**(5): 78-89.
- Edzwald, James K. and John E. Tobiasson. (1999) "Enhanced Coagulation: US Requirements and a Broader View." Water Science and Technology **40**(9): 63-70.
- Edzwald, J. K. (1993) "Coagulation in drinking water treatment: particles, organics and coagulants." Water Science and Technology **27**(11): 21-35.
- Gregor, J. E., C. J. Nokes, and E. Fenton (1997) "Optimising natural organic matter removal from low turbidity waters by controlled pH adjustment of aluminum coagulation." Water Research **31**(12): 2949-2958.
- Harms, Leland L. (1987). "Chemicals in the water treatment process." Water-Engineering and Management **134**(3): 32-34.
- Hawke, David J., Kipton J. Powell, and Jan E. Gregor (1996) "Determination of the Aluminum Complexing Capacity of Fulvic Acids and Natural Waters, with Examples from Five New Zealand Rivers." Marine and Freshwater Research **47**: 11-17.
- Krasner, Stuart W. and Gary Amy. (1995). "Jar-test Evaluations of Enhanced Coagulation." Journal American Water Works Association **87**(10): 93-107.

- Knocke, William R., Holly L Shorney, and Julia D. Bellamy. (1994). "Examining the Reactions Between Soluble Iron, DOC, and Alternative Oxidants During Conventional Treatment." Journal American Water Works Association **86**(1): 117-127.
- Knocke, William R., Sara West, and Robert C. Hoehn (1986) "Effects of Low Temperature on the Removal of Trihalomethane Precursors by Coagulation." Journal American Water Works Association **78**(4): 189-195.
- Kvech, Steve, and Marc Edwards. (2002). "Solubility Controls on Aluminum in Drinking Water at Relatively Low and High pH." Water Research **36**: 4356-4368.
- Langmuir, Donald. (1997). Aqueous Environmental Geochemistry. Prentice-Hall, Inc. Upper Saddle River, New Jersey.
- Lee, J. F., P. M. Liao, *et al.* "Behavior of Organic Polymers in Drinking Water Purification." Chemosphere **37**(6): 1045-1061.
- Licsko, Istvan. (1997) "Realistic Coagulation Mechanisms in the Use of Aluminum and Iron(III) Salts." Water Science and Technology **27**(4): 103-110.
- Licsko, Istvan. (1993) "On the types of bond developing between the aluminum and iron (III) hydroxides and organic substances." Water Science and Technology **27**(11): 249-252.
- Masters, Erika N. (2003). "Colloid Formation for the Removal of Natural Organic Matter During Iron Sulfate Coagulation." Thesis. Department of Civil and Environmental Engineering, Virginia Tech. Blacksburg, Virginia.
- Plankey, Brian J., Howard H. Patterson, and Christopher S. Cronan (1995) "Kinetic analysis of aluminum complex formation with different soil fulvic acids." Analytica Chimica Acta **300**: 227-236.
- Plankey, Brian J. and Howard H. Patterson (1987) "Kinetics of Aluminum-Fulvic Acid Complexation in Acidic Waters." Environmental Science and Technology **21**(6): 595-601.
- Powell, H. K. J. and D. J. Hawke (1995) "Free Aluminum and Aluminum Complexation Capacity of Natural Organic Matter in Acidic Forest Soil Solutions from Canterbury, New Zealand." Australian Journal of Soil Research **33**: 611-620.
- Ratnaweera, Harsha, Nicole Hiller, and Ulrike Bunse. (1999) "Comparison of the coagulation behavior of different Norwegian aquatic NOM sources." Environment International **25**(2): 347-355.

- Siczka, John S. (1997). "The Characterization of Dissolved Organic Material in Natural Waters and the Phase-Change Behavior of Organic Matter During Chemical Coagulation." Thesis. Department of Civil and Environmental Engineering, Virginia Tech. Blacksburg, Virginia.
- Singer, Philip C. (1994) "Control of Disinfection By-Products in Drinking Water." Journal of Environmental Engineering. **120**(4): 727-744.
- Snoeyink, Vernon L. and David Jenkins. (1980). Water Chemistry John Wiley and Sons, Inc., New York, New York.
- States, Stanley, Richard Tomko, Michelle Scheuring, and Leonard Casson. (2002) "Enhanced coagulation and removal of Cryptosporidium." Journal American Water Works Association **94**(11): 67-77.
- Tadanier, Christopher J., John S. Siczka, Duane F. Berry, and William R. Knocke. (1997). "The Influence of Dissolved Organic Matter-Colloidal Material Associations on the Application of Coagulation and Disinfection Processes to Natural Waters." American Water Works Association, Annual Conference.
- U.S., E.P.A. (1998). "National Primary Drinking Regulations: Disinfectants and Disinfection Byproducts; Final Rule. 40 CFR Parts 9, 141, and 142." Federal Register **63**(241): 69390-69476.
- Van Benschoten, J. E., J. K. Edzwald, and M. A. Rahman. (1992). "Effects of temperature and pH on residual aluminum for alum and polyaluminum coagulants." Water Supply. **10**(4): 49-54.
- Wang, Dongsheng, Hongxiao Tang, and John Gregory. (2002). "Relative importance of charge neutralization and precipitation on coagulation of kaolin with PACI: Effect of sulfate ion." Environmental Science and Technology. **36**(8): 1815-1820.
- White, Mark C., Jeffery D. Thompson, Gregory W. Harrington, and Philip C. Singer. (1997) "Evaluating criteria for enhanced coagulation compliance." Journal American Water Works Association **89**(5): 64-77.

VITA

William Michael Hardin, son of Gail Hardin and Michael Hardin, was born in Roanoke, Virginia on April 11, 1976. He earned his Bachelor of Science degree in Fisheries Science from the College of Natural Resources, Virginia Tech in December, 1998. He earned his Master of Science in Environmental Engineering from the College of Engineering, Virginia Tech in December 2003. He currently resides in Annapolis, Maryland where he works for Stearns & Wheler as an environmental engineer.